HHS Public Access

Author manuscript

ACS Sens. Author manuscript; available in PMC 2019 April 17.

Published in final edited form as:

ACS Sens. 2018 December 28; 3(12): 2475–2491. doi:10.1021/acssensors.8b01085.

Advances in Optical Sensing and Bioanalysis Enabled by 3D Printing

Alexander Lambert, **Santino Valiulis**, and **Quan Cheng***

Department of Chemistry, University of California, Riverside, California, 92521, USA

Abstract

The recent explosion of 3D printing applications in scientific literature has expanded the speed and effectiveness of analytical technological development. 3D printing allows for manufacture that is simply designed in software and printed in house with nearly no constraints on geometry, and analytical methodologies can thus be prototyped and optimized with little difficulty. The versatility of methods and materials available allows the analytical chemist or biologist to fine tune both the structural and functional portions of their apparatus. This flexibility has more recently extended to optical-based bioanalysis, with higher resolution techniques and new printing materials opening the door for a wider variety of optical components, plasmonic surfaces, optical interfaces and biomimetic systems that can be made in lab. There have been discussions and reviews of various aspects of 3D printing technologies in analytical chemistry: this review highlights recent literature and trends in their applications to optical sensing and bioanalysis.

Graphical Abstract

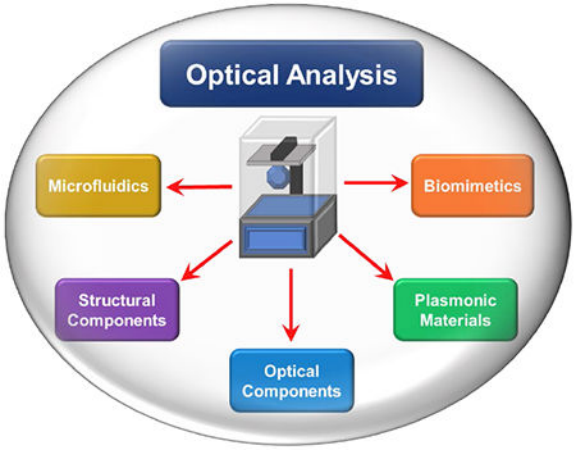

Keywords

3D Printing; Additive Manufacturing; Optical Sensing; Microfluidics; Surface Plasmon; Biomimetics

*Corresponding author: Quan Cheng, Tel: (951) 827-2702, Fax: (951) 827-4713, quan.cheng@ucr.edu.

The rapidly expanding interest in the general culture around 3D printing technologies over the past several years has mirrored its increasing use in academic research. The ease of use and relative low cost for manufacturing all manner of components for instrumentation enabled by the suite of 3D printing techniques has made the subject a hotbed for research, especially in analytical chemistry.[1] There are a group of manufacturing types that are categorized as 3D printing that will be discussed in this review that all share several similar core steps. One, they all use additive manufacturing in a sequential pattern, building the device layer-by-layer and fusing those individual layers into a contiguous whole. This is as opposed to subtractive manufacturing techniques, like etching, that take a block of material and remove pieces until the design is complete.[2] Additive manufacturing has the benefit of much less wasted material than subtractive methods. Second, they are usually designed in software, though some versions will convert images of real objects into software models first. The models are then converted into universally-recognized .STL files, which are sliced into the individual component layers by the 3D printer software before they are physically printed. Though there are a wide range of materials that can be used for 3D printing, the archetypal use is with plastic and polymer-based components, e.g. microfluidic designs for analytical techniques.

The software model-to-completed object process forms one of the fundamental benefits of 3D printing over older methods of lab component creation: ease of manufacture. Hot embossing and injection molding, two standard industrial techniques for plastic parts, are far too costly and inconvenient to set up practically outside of a large-scale purpose-built facility.[3] The dominant form of small parts manufacture in academic laboratories before 3D printing was soft lithography, the most common form of which involved molding and curing a viscous solution of polydimethylsiloxane (PDMS).[4,5] PDMS has many upsides, including excellent stability, chemical inertness, and good optical properties, but suffers if modifications are needed to the prototype. A mask or mold is required for the PDMS to be molded to, which must be machined via traditional methods like photolithography, and can be a costly and time-consuming process. 3D printing, on the other hand, requires only a few clicks of the mouse to change the model and reprint. Furthermore, complex internal structures are trivial to make in 3D printing that would be nearly impossible to the average user using previous methods. This ease of manufacture leads to so-called “rapid prototyping”, one of the most useful aspects of 3D printing, which allows a user to quickly optimize the component for their purposes.[6] PDMS still has several advantages over to 3D printing; most crucially, the resolution and subsequent component feature size that can be manufactured via a PDMS mask is much smaller (nanometer scale) than can be achieved with most current 3D printers (micrometer scale).[7] However, with the level of interest in 3D printing, improvements to the technologies are likely to equal or surpass the capabilities of PDMS-based soft lithography.[3]

Another central benefit of 3D printing is its ability to improve many aspects of point-of-care testing (POCT). Field labs without access to supply chains of the components of analytical instruments would only need a 3D printer and related materials to fabricate a variety of their own parts in a standardized way. Once equipped with this printing capability, many different sets of tests can be produced; all through the same device since all that is required is a simple file download.[8] Creating analytical methodologies using 3D-printed parts that can be

used for POCT constitutes a large portion of research and has great potential to make an impact on improvements in health outcomes around the world.

This review takes stock of current state of 3D printing technologies and their application to chemical and biological sensing methodologies (see Figure 1). Since any review that comprehensively covers every aspect of the expansive field of scientific 3D-printing applications would be exhausting, our focus will be on 3D-printing for optical sensing and bioanalysis. The similar use of 3D printing for electrochemical applications has previously been reviewed elsewhere.[2] 3D printing has become widely adopted as an aid for many types of analytical instrumentation. In academic settings, 3D printing is in fact becoming the standard form of parts manufacture and is frequently treated as a means to an end product, rather than as a prototype to be mass-produced at a later time. As such, rigorous study is underway in assessing the improvements to analytical methodologies that can be achieved with 3D printing. Topics as diverse as new complex designs for microfluidics, novel structures for electrochemical techniques, optical component manufacture, biopolymers, and whole instrument design are active research areas with 3D printing and point the way toward rapid improvements in the future.

METHODS OF 3D PRINTING

The types of manufacturing processes for creating 3D-printed structures are increasing at a steady pace in recent years. The complexity and sophistication of current techniques has also expanded as key patents on two major technologies (stereolithography and fused deposition modeling) have expired in recent years. Others suffer somewhat in their research interest due to still being under patent protection. Here, the major types of 3D printing techniques and their variations are presented in order of most relevance to current research directions.

Stereolithography (SLA)

The most foundational form of 3D printing in the modern setting is stereolithography.[9] The working principle begins with a working surface submerged in a reservoir of photocurable resin. A movable laser then polymerizes the resin at the working surface into a solid form; the stage is moved, and the process repeats. Each 2D layer solidifies and melds into the previous layer, creating a continuous solid object. There are two primary physical configurations for SLA, as seen in Figures 2a and 2b. The free surface, or bath, configuration, places the working surface at the top of the bath, and the stage is lowered for each successive layer.[10] The inverted “bat” configuration, or constrained surface configuration, instead places the working surface at the bottom of the reservoir over a transparent window.[11] The stage is raised with each layer, lessening the height restrictions and limiting the oxygen inhibition of the polymerization reaction because the working surface is submerged, significantly speeding up the curing time. Another advancement, CLIP, makes the bottom window oxygen permeable so that the lowest layer of the resin is oxygen-inhibited, preventing adhesion of the still-forming object to the window.[12]

Many alternate forms of SLA are used in the literature. A modification of the laser optics of SLA to a system known as two-photon polymerization (2PP) greatly improves the feature resolution, down to 10-100 nm with 2PP.[13,14] A femtosecond laser sends ultrafast pulses that

initiate two-photon absorption and polymerization on a very precisely targeted small volume of the photopolymer.[15] Of all the current 3D-printing techniques available, 2PP has the best resolution, and is appropriate to create high-quality optical surfaces and microstructures of considerable complexity. In digital light processing stereolithography (SLA-DLP), a digital micromirror is used as the laser source projector, which can simultaneously shine on and polymerize the entire working fabrication surface at once instead of scanning with a single source, significantly increasing build speed.[16] Other variations of SLA that have been developed and reported in the literature include modifications like substituting an IR-laser and thermally-curable substrates,[17] and adding multiple lasers in order to generate diffraction patterns[18].

Photocuring resins as a fundamental operating principle limits the range of materials that SLA-type systems can use compared to later techniques, as polymers such as poly(ethylene glycol) diacrylate (PEG-DA) or poly(methyl methacrylate) (PMMA) typify the type of materials used.[19] Additionally, care must be taken when fabricating small, enclosed channels within a larger microfluidic device, as lack of effective drainage of the liquid resin can cause partial solidification and distort the shape and size of the microchannels.[20] However, the good resolution and solid construction offered by SLA for instrumental components makes SLA the most standard method of fabrication for 3D-printed devices in research settings.

Fused Deposition Modeling (FDM)

The other major commercial version of 3D printing is fused deposition modeling, one of several techniques that relies on extrusion of materials to form each layer of the object.[21,22] As seen in Figure 2c, the desired material, initially in the form of a long filament, is pulled through a heated nozzle onto the working surface, where it binds with the previous lower layer in a semi-liquid form. The bonding between layers is fundamentally weaker for FDM than SLA because there is no chemical polymerization reaction to bond the layers. Sacrificial structural supports that can be removed later are frequently needed to prevent the collapse of voids during fabrication, the tradeoff being lower resolution, as removing the supports can be difficult and can leave unneeded material in sensitive areas. Industrial-level plastic manufacturing is able to bulk heat and reflow the plastic to improve its strength, and there have been more recently-developed FDM machines that include a heated chamber to simulate this effect in small scale while only marginally interfering with shape of the features.[23] The feature resolution of FDM is significantly lower than SLA and typically used to make channels on the order of 500 μm.[3]

The upsides of FDM as a primary 3D printing method are its versatility of materials and low cost. Since there is no fundamental chemical reaction in the fabrication, the range of materials available is much wider, with standard filaments available of many industrial materials like acrylonitrile butadiene styrene (ABS), poly(lactic acid) (PLA), polystyrene, polycarbonates, poly(ethylene terephthalate) (PET), poly(vinyl alchohol) (PVA), and polyamide (or Nylon),[24] polycarpolactone (PCL), polylactic acid (PLA), polybutylene terephthalate (PBT) and polyglycolic acid (PGA).[25] And since the filaments come out of re-positionable nozzles, multiple nozzles can be outfitted to the device, allowing for multi-material printing.[26] More recent variations of FDM are able to extrude “cold” materials that

are in a more liquid form at room temperature. This version, also known as robocasting, is capable of using an even wider range of materials, including ceramics, metals, hydrogels and other biopolymers, with the tradeoff being that there are usually some post-processing steps to improve the structural integrity.[2] An FDM printer itself is typically much less expensive than SLA, which is important if the analytical techniques are to be used, for example, in point of care testing (POCT).[6] Similar in flexibility and price is laminated object manufacturing (LOM), which uses laminated sheets of nearly any material that are cut by a laser and then bonded together either chemically or by hand.[27] LOM also suffers from low resolution and is not commonly used in academic settings.[3]

Inkjet Printing

Inkjet is an umbrella term for several relatively newer variations of 3D printing that are united by the common feature of using the pre-existing mechanical architecture of ink printers to trace the active layer of fabrication.[28] In the powder-based version, also known as binder jetting, the printer deposits lines of adhesive or photopolymer in a pattern that is then hardened through physical (heating) or chemical (UV light) means (see Figure 2d), creating a final material that is a blend of the polymer and powder.[2] The stage is lowered, new powder is rolled onto the active surface, and the process is repeated layer-by-layer. Photopolymer inkjet uses multiple printer heads to deposit a photopolymer and support material simultaneously that can be photocured by a broad UV light source between each step.[29] This technique is also known as polyjet or multijet depending on the type of support material.[14] The resulting structures in photopolymer printing are relatively low-strength because no pure material is being used, and fabrication frequently requires support structures.[30] The resolution and surface roughness of inkjet printing is comparatively good, [31] with some models reaching resolutions of less than 20 μm.[32]

Inkjet, especially of the photopolymer type, is very capable of multi-material and multi-color printing,[33] and are perhaps the best 3D printing techniques available for dense, complex microfluidic super-structures. A barrier to development of analytical chemistry techniques is the lack of knowledge of the photopolymers themselves, as they are all proprietary materials. Though many companies market a wide array of polymer/powder combinations with various physiochemical properties,[34] academic research groups are limited in their ability to design functional experiments and surface chemistries around them.[14] Though relatively more expensive than most other techniques due to the proprietary nature of the materials, inkjet-type technologies are high-performance in total, and are an excellent area for future potential development.

Selective Laser Sintering (SLS)

Selective laser sintering was the first powder-based 3D printing technique, using a high-powered Nd:YAG or CO_2 laser to selectively sinter or melt a fine powder at the active fabrication surface in the .STL specified pattern.[35] The stage is then lowered, and a roller from an adjacent powder container respreads a new layer onto the surface for the next layer, as seen in Figure 2e. The resolution is low-to-intermediate, around 100 μm, and is fundamentally determined by the particle size of the active layer and the focus spot of the laser.[36] Of the main categories of 3D printing types, selective laser sintering is the one that

comes the closest to matching the strength of standard industrially-fabricated parts, and the products usually retain the properties of the bulk materials.[22] Components made of metal or metal alloys are the best suited to SLS (or selective laser melting, SLM, as it is termed when the powder material is only metal), as SLS is similar in the microscale to how metals are worked in larger settings. The sequential addition of new layers of powder makes SLS quite capable of multi-material printing, adding extra levels of complexity to a design.[37] Significant limitations for printing polymer microfluidic or optical components arises from unsintered material that remains on the surface or in small channels, along with the higher inherent surface roughness of the technique.[38]

Direct Printing

Some various remaining, largely straightforward, methodologies for 3D printing, i.e. ones that simply directly place the desired building material on the surface with few additional steps, are usually categorized under the general terms of direct printing, direct writing or direct ink writing.[1,3,4] The general form of the techniques is that they are extrusion-based, printing a line of the material in a pattern with or without a .STL file. The printer is typically built or designed for a specific application, or the various fabrication parameters are home-modified on a standard FDM-type instrument. Nozzle size, temperature, extrusion speed and horizontal scanning speed can all be adjusted to fit the particular experimental needs of the user, and some-post processing steps may be added. The specific application can be tuned for very precisely, which makes the concept appealing for researchers creating new systems and instrumentation. On the flipside, direct ink printing eliminates the possible upside of 3D printing that parts and analytical methodologies can be standardized and used across vastly different environments.

Bioprinting is one of the most prominent areas of direct printing. Hydrogels and cell solutions are typical materials that are extruded through a printer mechanism in a pattern of biological significance, such as in the shape of a particular tissue or organ.[39] Some setups may combine this technique with a standard photocurable resin to serve as a scaffold to set the ink solution in place.[40] 3D-printing of these biostructures has appeal because the materials used can be varied to create different optical properties that either conform more closely to the biological model or make analysis of the biostructure easier.[41]

OPTICAL APPLICATIONS OF 3D PRINTING

Optical Sensing with Microfluidics

There has been a proliferation in the literature in recent years of microfluidic architectures that use 3D printing due to the ease of manufacture of complex and customized internal designs. A typical example was presented by Santangelo et al.[42] Multiple geometries were combined and fabricated with an SLA printer, as depicted in Figure 3a. Multiple inlets for a luciferase ATP bioluminescence reaction were injected, led through a mixing channel to a reaction chamber optimized for optical signal collection by adjacent photomultipliers, followed by a product outlet line. 3D-printed systems can also be integrated with separate flows for specific reagents at different points in the experimental design, as seen in Mattio et al (Figure 3b), where 4-(2-pyridylazo)-resorcinol (PAR) was added to a sample after a

preconcentration step in order to elute lead.[43] Microfluidic systems like these would be extraordinarily difficult to prototype by other means than 3D printing, and the final product of a 3D print tends to be a unibody design, minimizing fault points.

Extensive study has been conducted into fluid movement via valves and pumping through 3D printed microfluidic devices,[20, 44–45] which have previously been reviewed.[5, 14] Droplet generation within a microfluidic system is also an active area of research.[46,47] Several recent analyses have also shed light on the dynamics of 3D printed microfluidic architectures. Gelber et al analyzed the effect on reagent mixing within the channels of a helical 3D-printed device with large numbers of turns. They used both simulations and stimulated Raman scattering on printed substrates to develop a model for analyzing the actual mixing profile within microfluidic channels.[48] A recent study compared the mixing efficiency, feature size, and surface roughness of microfluidic Y-junctions printed by several 3D-printing the subsequent effects on device applications. Their extensive analyses concluded that FDM was best suited for micro-mixers, Polyjet was most applicable for cell culture platforms and droplet generators, and DLP-SLA was the highest-performing for pure microfluidics.[49] Li et al studied fluidic behavior in FDM-manufactured mixing channels, the results of which indicated that the angle of filament extrusion has a significant effect on mixing behavior. Much more mixing was observed when the filament was at a diagonal angle (60°) to the flow direction, rather than 0° or 90°.[50]

There are a wide variety of microfluidic 3D printing applications that use optical sensing. In fact, for analytical chemistry, microfluidics is essentially the dominant current application, as many further electrochemical or optical applications frequently include microfluidic portions as well. This discussion of optical methods via microfluidics is grouped into several subcategories that concern different design features of the optical sensing devices.

Optical Detection

The relatively recent advent of commercially available optically clear resins has led to wider development of microfluidic designs that rely on direct colorimetric analysis after multiple preparation steps. A typical example comes from Shallan et al, who reported a complex microfluidic gradient system that uses a transparent polymer as the body printed from a standard SLP printer (Figure 4a).[51] This enabled visual detection of nitrate in water using a colorimetric Griess test: the channels created a standard addition calibration for the sample, and the intensity data via single-line spectrophotometry. The sensitivity of this methodology was comparable to standard spectrometer-based detection, so the optical quality of the polymer was strong enough for this application. Multi-material FDM printing was recently used to construct another microfluidic system for a colorimetric Griess test. In this case, dual nozzles were able to print the flow cell in conjunction with a porous membrane, which helped to facilitate ion transport.[26] Chan et al was able to create a colorimetric detection system that used almost entirely 3D printed parts. The design included a manually actuated pump and multiple valves that moved the liquid flow past several chambers of reagents (Figure 4b). The system was able to optically quantify urinary protein at physiologically relevant levels.[52] Sheath flow was utilized to focus a sample stream into a small space for micron-scale particle counting via optical fiber (Figure 4c). The setup was able to

distinguish between particles of different sizes and could effectively count up to 5.5×10^4 particles/mL.[53]

Luminescent optical detection methods have been regularly coupled to 3D-printed microfluidic devices in a variety of ways. The general setup is that the target analyte is flowed into a sensing chamber, and the luminescent tag is attached to the analyte as end step or during the sample prep portions of the device. Tang et al printed a complex unibody design with SLA that attained excellent sensitivity, down to 0.5 pg/mL, for multiplexed detection of cancer biomarker proteins using a standard chemiluminescent detection system. As seen in Fig 5A, successive reservoirs introduce the various reagents, followed by a dense network of mixing channels, leading to a detection region where the optical chemiluminescent signal was collected by a CCD camera. This design benefits from smooth integration of the segments of the unibody design (requiring only a single inlet pump for operation), one of the primary features of 3D printing.[54]

A setup utilizing electrochemiluminescence (ECL) was reported for multiplexed detection of prostate biomarkers. The gravity-based SLA-printed flow cell array adds (RuBPY)-doped silica nanoparticles to immobilized antigens that are activated by an adjacent supercapacitor, and the resulting ECL signal was also collected by CCD camera. The flow cell itself was also integrated into a larger 3D-printed module that could lever the array up into “loading” position and down into “wash” position flowed the analytes for analysis (Figure 5b). The system attained detection limits of the biomarkers that were comparable to ELISA.[55] These examples effectively showcase benefits of 3D printing for optical analytical detection systems: the ease of integration of several parts, small materials cost, and requirement of only a CCD camera for detection that make up.

Mechanical Integration

Though there are fully-packaged 3D-parts-only detection schemes, the ability to integrate with electronics is an important feature of 3D-printed designs, as more complex and flexible sequences of fluid movements will require automated control. Several recent examples in the literature indicate the possibilities of such an approach. An automated ECL array was used for multiplexed detection of up to 8 different proteins in human serum. Using a sandwich-assay design, the 3D-printed microfluidic cell introduces the sample and reagents by passing them over a single-walled carbon nanotube that could then be activated to generate the ECL signal (Figure 6a).[56] Another automated system used ECL to evaluate the DNA damage instigated by environmental inputs like cigarette smoke. The environmental factor was introduced to films of metabolizing enzymes and DNA in a microfluidic cell. The detected ECL reaction was based on guanine, so if the environmental factor damaged the DNA, guanine was released and ECL signal increased. Genotoxicity profiles could be developed for many potentially harmful factors via wide distribution of this platform.[57]

An intriguing mechanical integration with 3D-printed optical detection has been developed by Bauer et al. Extensive prototyping enabled by FDM 3D printing created an ELISA-based detection platform for malaria. The disposable microfluidic cartridges are connected to a series of servos and actuators to control the fluid movement (Figure 6b). The system can be adapted for multiple assays because the interface uses audio files to control the steps, with

different “songs” playing different steps of frequencies that the pumping system interprets for different actuation steps. Since the system can essentially be controlled through an audio jack, this has significant potential for point-of-care applications.[58]

Frequently, these microfluidic designs are combined with smartphone camera for the light detection so that the system can be used for point of care applications. This takes advantage of the ubiquity of smartphones in the developed and developing worlds; if the detection system is optical and based on visible-range light, then everyone with a smartphone camera is carrying around a potential spectrometer in their pocket. However, many optical analytical methods, especially luminescent ones, have such a low signal compared to ambient light that a simple point-and-click would not suffice. Instead, the structure, microfluidics and pre-optics are packaged into a cartridge that can be attached around the camera itself, limiting the background ambient interference. Roda designed a one-step, three-chamber microfluidic accessory that could be adapted for various luminescent assays. Both a luminol-H_2O_2-HRP chemiluminescence assay for cholesterol and a luciferase-based bioluminescence assay for bile were integrated into the accessory and produced clinical relevant detection limits for each.[59]

Ko et al manufactured an ELISA-based device that was able to target the exosomes in cerebral spinal fluid that are produced by the brain after a concussion. Indicator exosome antibodies were attached to enrichment microbeads that, after picking up the targeted exosome in the microfluidic channel, passed through a micropore filter into a detection chamber where the ELISA reagents were added (Figure 6c). Background exosome antibodies were attached to much larger microbeads that could not pass through the filter to the detection chamber, reducing the background optical signal from the ELISA assay. The total analysis via this compact 3D-printed method is much faster than clinical analysis of exosomes which requires time-consuming sample preparation.[60]

Sample Pretreatment

A constant challenge for optical analytical techniques is being able to sense an analyte through a complex matrix. Preconcentration and separation are ways to make sure the target molecules at the detector are the primary ones around, and 3D printing has been used to this effect numerous times. For example, Liu et al printed a clamshell-case design via SLA and added hydrophobic coating to use as a plasma separator. After separation of plasma from whole blood, they were able to detect the DNA of the parasite *S. mansoni* with good recovery via the LAMP method and fluorescent detection.[61]

Magnetic particles as a means of preconcentration is a common tactic in microfluidic designs. A typical example was presented by Lee et al, where multiple geometries were combined and fabricated via SLA (Figure 3c,d). Magnetic nanoparticles were attached to *E. Coli* via an antibody in a sample, then separated with magnetic field enhancement in the helical chamber, then outflowed for optical UV-Vis absorbance detection. Detection of *E. Coli* was 10 cfu/mL in buffer and 100 cfu/mL in milk.[62] Park et al also used an Fe_3O_4-anitbody conjugate to bind to *E. Coli*, which were then collected directly at the bottom of a helical chamber. Instead of UV-Vis, detection was carried out by an ATP luminometer, resulting in a detection limit of 10 cfu/mL in blood (Figure 7a).[63] Ganesh et al designed

multi-chamber microfluidic device for *E. Coli* detection that concentrated the magnetic nanoparticles in one chamber before outflowing to a polymerase-chain reaction (PCR) chamber, which was then collected and analyzed via gel electrophoresis and fluorescence.[64]

An even wider array of functionalities is enabled by the microfluidic device designed by Han et al to analyze messenger RNA in blood. The mRNAs are complexed to magnetic beads and then passed across a magnetic microfluidic channel to separate the mRNA from the blood matrix and into a separate chamber (Figure 7b). From there, more reagents are flowed in for both synthesizing complimentary DNA (cDNA) from the mRNA, and then amplifying the cDNA via PCR. The DNA was subsequently fluorescently labeled and analyzed, providing important analyses of a very relevant biomolecule with only a very small required sample volume.[65]

In the same vein, extractions and chromatographic-type separations have been carried out by several groups. The lack of fine surface control in most current 3D printing techniques hampers the ability to make finely porous surfaces needed for more intensive separations. Instead, membranes or sorbent materials can be attached to or inserted in the channels. For example, Kataoka et al were able to extract petroleum compounds from their briny native solutions using a solid-phase extraction (SPE) sorbent packed into a simple FDM-printed microfluidic chips, which could then be sent on for further analysis.[66]

Calderilla et al have reported multiple versions of an extractor for optical metals testing that inserts a standard commercial solid-phase extraction (SPE) sorbent disk within a complex microfluidic system printed with SLA that can support reagent and eluent lines. Iron was directly detected, both in the form of Fe(III) and total iron after the addition of an oxidant. The two different analyses from the same microfluidic system were enabled by the multiple channels built into the device, which was ultimately more easily designed and integrated because of the nature of 3D printing.[67] Similarly, in the other system, chromium was complexed via a reagent line before detection, and both setups used optical analysis via single-line spectrophotometric detection.[68]

Even with the present lack of fine surface control, some researchers have managed to use the polymer material for extractions. Solid phase extraction configurations using only 3D printed components have been reported for trace metal analysis that can be coupled to various instrumentation. Su et al fabricated a microfluidic device made of a polyacrylate polymer that included an extractor/preconcentrator chamber made of cubes of the same material that functioned as a solid phase extraction column. The resulting detection of trace metals in seawater that was on par with traditional extraction techniques.[69] Belka et al was able to print a thermoplastic elastomer-PVA composite that was able to extract drug-like compounds from water samples.[70]

In addition, some separations and optical chromatography using 3D printed parts have recently begun emerging, especially using thin-layer chromatography. One example printed silica gel layers via modified FDM into an array of 40 microfluidic channels that was able to run planar chromatography to separate colored dyes with excellent resolution.[71] Another version used polyjet printing to create a smaller set of channels to use in the separation of

both colored dyes and fluorescently tagged proteins myoglobin and lysozyme.[7] The benefit of both methods is the much easier materials manufacture over conventional chromatography plates.

In all of the above separation examples, no additional surface coating was used beyond the 3D-printing steps. Surface functionalization via chemical means for the purpose of separations depends on the material, and many top-of-the-line 3D printing devices use proprietary polymers whose surface properties are not very well characterized.[14] Gross et al overcame this problem by coating a polyjet-printed fluidic channel in PDMS and polystyrene to improve cellular adhesion before lysis.[72] Several different polymer, metallic and dielectric coatings were analyzed by Paknahad et al on polyjetted microfluidic channels for gas-phase sensing, and found that a bland of chromium, gold and Parylene C showed the best selectivity.[73] Silane-coupling agents (SCAs) have been used in multiple methodologies: Ohtani et al coated a fluorinated SCA to a silica-coated SLA polymer to create a hydrophobic surface,[74] while Song et al bonded SCAs of varying functionality to Al_2O_3 ceramic particles that were then used in the SLA printing of various objects to improve structural integrity.[75] Epoxy-based resins are frequently used in 3D printing,[76] whose hydroxy groups can be used for a wide array of derivatization chemistry for surface functionalization.[77] Notably, Credi et al recently printed sensing channels using biotinylated polymers for various analyses via optical microscopy.[78] The biotin-avidin binding interaction is frequently used in optical methods to scaffold various functionalities together, so this type of embedded surface functionalization would widely versatile applications for biomolecule detection.

Optical Components

As technical instrumentation becomes more complex and specialized, there is an increasing interest in printing not only the flow channels and structural components of analytical devices, but also the optical couplers that are used for analysis. The utilities of optical coupling components like prisms, lenses and waveguides are greatly improved if they can be adapted to a specific use-case, and fast-prototyped in a similar fashion to other 3D-printed components of a system. This has led to the growing study of the 3D-printing of optical components.

One of the primary advantages of PDMS over 3D printing is the high optical quality of PDMS parts that can be integrated into optical analytical systems. For lab-made optical and components like prisms and lenses, one standard strategy is to 3D print a mold that is used to make the higher-quality PDMS optical component such as a prism.[79] The sources for this quality are twofold. First, due to feature resolution being much better for PDMS than 3D-printed structures, the surface is much smoother for PDMS, reducing unintentional scattering and signal loss from the light source.[80] Second, the material of PDMS is naturally optically clear, with a refractive index of 1.4, which approaches that of borosilicate glass.[81] The most widespread 3D printing techniques often use opaque or near-opaque polymers which totally inhibit optical properties. The first advantage will naturally dissipate over time as the quality and resolution of 3D printing techniques improves, but both are areas of active research, and several developments have sought to close the gap in one of two ways: by

improving the technology for directly printing glass itself, or by improving the optical qualities of standard 3D printing polymers.

Optical Components via Polymer Printing

The recent development of commercially available transparent polymer resins[82] has enabled the basic form of optical components to be printed with refractive indices in the range of commercial glass. Luxexcel uses a proprietary form of inkjet manufacturing to offer a range of custom printing of transparent optical components[83] that have surface roughness on the order of 10 nm,[84] which is suitable for many optical applications. For users who want to keep designs in-house in order to maximize the fundamental flexibility and rapid-prototyping of 3D printing, one of the central difficulties still to overcome is resolution. The most common techniques, such as SLA and FDM, produce components with surface roughness that disperse too much light to be effective optical couplers. The technique that does not suffer this problem of resolution is two-photon polymerization, and there are many examples of 2PP being used to print optical components, and like multi-lens objectives and free-form coupling elements (Figure 8a) that will have many applications for analytical sensing.[85,86,87] The excessive timescale of 2PP manufacturing, ~100 days for 1 mm^3,[88] means that it is limited to microstructured components, however, and may have difficulty becoming a widespread technique for academic labs who want to prototype macro-scale instrumentation.

Post-processing steps are a straightforward path for improving the surface roughness of printed components. Comina et al have printed systems of optics (lenses, prisms, etc.) with SLA-DLA to be used in a smartphone accessory for fluorescence- and chemiluminescence-based optical detection.[89,90] They were able to generate a smooth surface by adding a thin coat of resin to the optical surface after printing and letting it dry, filling in any imperfections (Figure 8b). This process improved the surface roughness from ~150 nm to ~7 nm. Vaidya et al also added a thin layer of resin coating as a post processing step to produce a surface smooth enough to metallize for mirrors and solar concentrators (Figure 8c). Their smoothing process reported an improvement in the surface roughness of SLA-printed objects of ~70 nm to 2.3 nm.[91] Polishing the surface by hand has been shown effective at improving the surface quality of 3D-printed parts to ~20 nm, a level suitable for some optical instrumentation.[92] Dewey et al have demonstrated the use of IR laser polishing to improve the surface roughness of FDM-printed parts. They decreased the surface roughness to 2.0 μm along with improving the overall structural integrity of the object.[93]

Terahertz waves, as incorporated into sensing platforms, do not require a high surface smoothness because of the long wavelength (1 mm to 100 μm) of the incident radiation. This makes them a natural fit for easy integration with current-quality 3D printed parts. THz spectroscopy has the capability to monitor optical properties of thin films and distinguish specific spectra of solid powders, and there have been a number of reports of 3D printing the optical components required for THz wave sensing. Using both SLA and FDM printing of polymers, several groups were able to print high-quality waveguides,[94,95] diffraction gratings,[96] prisms,[97] and lenses[98] that could be used for optical analytical sensing. Because

of its flexibility in surface substrate, THz-based sensors could provide a platform for that packages well with 3D printing for field testing purposes.

Optical Components via Glass Printing

Glass would be the ideal material to 3D print for optical components, as it is more structurally and chemically stable than polymers and have higher transmission in the UV and IR regions.[99] However, glass has been one of the more difficult materials to 3D print, due to the high temperatures needed to soften it enough to work with (>1000 °C) and its quick hardening upon exposure to lower ambient temperatures. As a result, most research until recently has only been able to produce transparent glass for decorative purposes.[100] The quick cooling makes the final product ribbed, and so not suitable for optical measurements. There is also substantial research into 3D printing of bioactive-glass,[101,102] which is used for structural biological components, but this glass is non-transparent.

Several hybrid 3D printing methods have recently been developed for glass manufacture. They generally take the form of suspending silica particles in a 3D-printing resin or ink, printing the object by extrusion, then decoupling the resin or ink from the silica via a high-temperature sintering step, leaving the fused silica object. Kotz et al used silica nanoparticles dispersed in a hydroxyethylmethacrylate (HEMA) polymer that was used for standard SLA printing. This was followed by a two-step heating process to first decouple the polymer from the particles then to fully sinter the glass at 1300 °C, which resulted in very uniform glass objects, as seen in Figure 9a.[103] Cooperstein et al demonstrated a sol-gel based process using a 3-acryloxypropyl trimethoxysilane (APTMS) precursor to print, dry, then heat fused silica glass. By varying the percentage of APTMS and the temperature of the final heating step, they were able to tune the refractive index of the produced glass. They also added a polishing step at the end that reduced the surface roughness to 5 nm, well within precision grade standards for glass.[104] Destino et al were also able to tune the refractive index of the printed glass by synthesizing core-shell TiO_2-SiO_2 nanoparticles with varying titanium percentages (Figure 9b).[105] Nguyen et al used fumed silicon nanoparticles suspended in tetraglyme in a direct ink writing set up for the structure printing. They also suspended gold nanoparticles in the ink, doping the glass with a red color, opening the door for more complex hybrid materials.[106]

Alternatively, Luo et al have used a CO_2 laser in an SLM-type manufacturing method to locally melt both glass[107] and quartz[108] filaments in the desired layer pattern. The process takes place on a heated build platform, which mitigates the quick hardening, and therefore the ribbing in the final product. They were able to print optically transparent components including a lens-type object with good surface smoothness after polishing. Temperature variation at the laser-filament interface had a large effect on the final product, as too high of a temperature produced bubbles between the filaments, and too low of a temperature did not reduce the ribbing enough. This and the previous methods are all promising steps towards being able to 3D print glass directly in the lab for many types of components, optical and otherwise.

Plasmonic Surfaces

Plasmonic surfaces are a subject of growing interest in the areas of materials and sensing interfaces. Fundamentally, an incident photon beam excites a propagation of surface plasmon polaritons, or the plasmonic response, that is controlled by the interaction of the materials at the surface interface.[109] Most commonly used with noble, less oxidizing metals like gold and silver to simplify the surface chemistry, the plasmonic response is configured in multiple ways to probe the nature of the molecules in contact with the plasmonic material. Because of the complex and technical nature of using manipulating plasmonic responses, only recently have 3D printing applications begun emerging that take advantage of this type of effect. As previously discussed, 20 nm gold nanoparticles were coped into a sol-gel matrix for glass printing to generate a SPR coloring response.[106] Haring et al suspended silver nanoparticles of varying sizes (15-79 nm diameter) into both Pluronic F-127 and poly(ethylene glycol) diacrylate (PEGDA) to create “plasmonic inks” that were deposited via extrusion into a variety of constructs (Figure 10). The varying plasmonic responses were clearly distinguishable in different regions of objects, and finely graded surfaces transitioning one particle to another were also demonstrated.[110] The manufacturing flexibility of 3D printing makes complex surfaces like these much more feasible for an academic researcher.

Analytical sensing via plasmonic interfaces most commonly takes the form of surface plasmon resonance (SPR) spectroscopy, which has the benefits over luminescent optical detection methods of being label-free and real-time.[111] 3D-printing has begun to find application to SPR techniques. A common combination of 3D printing and SPR is in the printing of custom parts for integrating an SPR system to a specific situation. A 3D-printed stage and flow-cell were printed by Hwang et al to integrated with a SPR sensing configuration for the transdermal monitoring of cortisol.[112] Zhang et al recently used FDM to print the entire assembly of structural components and holders for the individual functional components of an SPR spectrometer.[113] A smartphone accessory was 3D printed for interfacing with a biosensing array that uses the higher-throughput version SPR known as SPR imaging.[114]

An exciting advancement was recently demonstrated by Hinman et al. for SPR biosensing with the optical components being 3D printed[92]. Equilateral prisms were printed via SLA and polished, followed by gold deposition on the prisms which served as the plasmonic surface for a standard Kretschmann configuration setup (Figure 11). The system was able to detect cholera toxin with good sensitivity after attachment of a tethered lipid bilayer and GM1 for capture. Gold nanoparticles were also grown on the surface of a dove prism via polydopamine for use in the single-axis configuration of SPR.[92] The benefit of 3D printing in this case is that the optimization of the experimental setup can tilt in more than one direction: the optical configuration can be optimized to the rest of the system rather than the rest of the system having to comport to the available optical components. Flexible optical applications like this are likely to become more common as 3D printing becomes more widespread in academic environments.

Electron beam-based 3D printing is another form of additive manufacturing that is used in varying forms to manufacture both macroscale[115] and microscale[116] objects and has recently

been applied to the design and fabrication of novel plasmonic structures. Winkler et al have used a custom direct printing technique based on focused electron beam induced deposition (FEBID) to print a range of nanoplasmonic architectures. Gold is the most commonly used plasmonic material, and it was used here to build up a range of designs with high plasmonic sensitivity.[117] FEBID is applicable to many plasmonic materials, and has been used to manufacture silver and platinum plasmonic nanostructures.

Other groups have investigated plasmonic-type interactions with 3D-printed substrates in various ways. Pandey et al used polyjet to print a terahertz region waveguide that was then covered in a layer of deposited gold for plasmonic sensing.[95] Lee et al used modeling to investigate the possibilities of using Fano resonance, a subtype of plasmonic response, on 3D polymer substrates, and found that hollow dielectric resonators would be suitable components.[118] In an intriguing coupling of 3D printing and plasmonic effects, Gupta et al used a custom printer setup to print core-shell spheres of poly(lactic-co-glycolic) acid (PLGA) that could be loaded with 25 nm diameter gold nanorods. The nanorods heat up upon laser exposure due to a strong localized surface plasmon resonance (LSPR) response. This thermal energy transfers to the polymer, bursting the spheres and selectively releasing a biomolecule payload that is monitored with fluorescence.[119] More types of plasmonic interactions will be likely be applicable to 3D printing in the future as the technology further develops.

Structural components

In addition to the designing of optical components with 3D-printing, structural components can also be created to offer precise and complicated arrangements for conventional optical equipment. These pieces indicate the true flexibility and utility of 3D-printing in the lab, as any design can be aided in its implementation by fully-customized parts. One such example by Wang et al, coupled a 3D-printed platform with a smartphone for optical detection of herbicides. A prism array and mirrors are supported by a 3D printed structure that also provided the necessary black box for optical detection. The compact 3D printed black box was then applied as an optical sensor for the detection of herbicide 2,4-dichlorophenoxyacetic acid. The assay functions based upon a competitive ELISA, and the blue color is produced from the HRP reaction. The blue color can be detected by the phone's camera and results are comparable to that of a laboratory microplate reader.[120] In a similar vein, Cevenini et al developed a toxicity biosensor based upon bioluminescent kidney cells. The cells were placed in 3D printed cartridges and placed into a 3D printed black box that was designed to attach cleanly to a phone. The phone could measure the bioluminescence which was proportional to the toxicity of the sample injected.[121]

Structures more akin to traditional microscopes can also be fabricated using 3D printed supports. A support was built for a digital holographic microscope (DHM), which is used in biological imaging and allows for the length and height of a cell to be measured. The 3D printed nature of the structure allows for the most compact instrument design to be made and quickly prototyped. This was applied by Javidi et al to detect sickle cell anemia in blood samples. Sickle cell anemia causes cells to become elongated because of a mutation in the hemoglobin, this can be seen using DHM.[122]

Fluorescent microscopy can also be arranged with 3D printed structures. Pandey et al use total internal reflection fluorescence with a compact 3D printed arrangement to measure the fluorescence of model systems such as latex beads and mammalian cells. The 3D printed structure is designed to fold into itself, and the optical components can be freely exchanged to meet the needs of the system.[123]

Biosensing can also be applied to heavy metal detection through urease activity. However, problems arise as multiple heavy metal ions can activate the enzyme, which would disrupt the validity of a calibration curve. Similar to the previous examples, a 3D printed platform was designed that attached to a smartphone, whose camera was used as the spectrophotometer. The platform can even be attached to multiple phones based upon an adjustable hook system. The system was designed to house a standard glass cuvette for the measurements.[124]

Flow cytometry relies upon the advantages provided by glass when compared to 3D printed polymers, but integration of 3D printing can still be beneficial. The glass micropipette is properly aligned into the optical arrangement necessary for the flow cytometry measurements.[125] As previously discussed, microfluidic chips are frequently designed by 3D printing techniques, and Driesche et al made a 3D printed holder for a non-3D printed microfluidic chip. They combine the precision of silicon chips with the customizability of 3D printing to take advantage of both. When low resolution is acceptable, 3D printing is the preferable method of fabrication because of its ease of use. In addition, the 3D printing allows for the platform to match the necessities of a variety of microfluidic chips. They take advantage of this and combine traditional glass or silicon chips and 3D printed holders with further integrated electrical systems and fluidic connections. Along with the fluid connectors, an integrated system for fluorescent measurement can be arranged to receive signal from the microfluidic chip.[126]

3D printed real time PCR devices can also be made. In this case, the individual components of the PCR, such as the thermocycler, were placed into a 3D printed structure with a custom-made fluorescence optical setup (Figure 12). Real-time PCR or qPCR is advantageous because it allows for more quantitative results to be found compared to normal PCR. The compact qPCR facilitated by 3D printing could then be transported to countries where laboratory equipment is not available. The qPCR was validated by using an intercalating fluorescent dye, 6-FAM, that will allow for the fluorescence intensity to increase proportionally to the DNA amplicons. The 3D printed qPCR exhibited lower efficiency of 79.10% compared to an 93.11% efficiency demonstrated by conventional qPCR. The authors attributed to unoptimized reaction conditions, and that with optimization it could be comparable.[127]

Optical Biomimetics

Biomimetics is a growing field that looks to replicate biological systems using non-biological materials. Inherent difficulties with fabrication of biomimetics such as the specificity necessary to replicate a unique organism and expense of materials limits their usage. 3D-printed biomimetics is a promising field, as the nature of 3D-printing allows for rapid experimentation that couples effectively with the complexity of biological systems.

Similarly, 3D-printed materials can also easily be changed to better resemble biological systems. The materials used can be varied depending on the goals of the biological emulation. One example of this is in the creation of biological phantoms, full scale 3D-printed replicates of a piece of anatomy.

One such neurovascular phantom was used to analyze the viability of near-IR fluorescence sensing in the human brain. The material used in the 3D-printing process optically replicates the complex human brain. Liu et al constructed a 3D image of a brain for use in 3D-printing based upon MRI images of a patient. The images were used to form a volumetric image with distinct tissue types. In the study, the grey matter, white matter, veins and arteries were focused on. The original 3D-printed phantoms required size modification of some vasculature to an average size of 1.7 mm, with a manufacturing resolution of 0.1 mm. The materials used were determined by matching testing the scattering of light through different slabs, and one was found to closely match the cerebral optical properties. Compared to a conventional rectangular phantom, the modeled brain phantom provides a better signal to noise ratio because the amount of material between the detector and the fluorophore was reduced. As shown in Figure 13, near-IR fluorescence can be seen through the phantom where the fluorophore was present in the vasculature.[128]

Whole organism phantoms can also be created to determine the effectiveness of deep tissue fluorescence. A mouse phantom was created by Bentz et al. Similar to other methods of changing the refractive index, they used a combination of the clear photopolymer and polystyrene beads that effectively could cloud the clear polymer and allow it to match the refractive index of whatever system was mimicked. To prove this concept can effectively replicate a biological system, a mouse phantom was created with cavities that represent what are the organs of a mouse. Frozen EGFP, a fluorescent protein, was placed in the brain cavity and was used to verify the biomimetic nature of the phantom via fluorescent optical diffusion tomography. Similar to the mouse phantom, a mouth phantom was also created that used the same fluorescent techniques to determine inhomogeneity in the tissue. This could be used to find ruptured blood vessels.[129] Dempsey et al created an infant head phantom and utilized optical techniques to verify its capabilities as a replica for possible further use. However, the material used for the phantom created was homogenous throughout the system, limiting the biomimeticism.[130]

Diep et al looked to improve on this shortcoming and developed a dual printed phantom. The extruded filament either took advantage of dyes or TiO_2 powders to modify the optical properties in different regions. The phantom which mimicked a real mouse with prostate tumor was found to have optical properties matching the real mouse, within 3%. The authors reported that improvements still need to be made, as the phantoms absorb more light in the visible range than their biological counterparts.[131]

A 3D printed tactile sensor was also developed by Ward-Cherrier et al. The so-called Tactip aims to replicate the tactile detection of a human finger. In the Tactip, the camera mount and the rigid part of the tip are 3D printed in addition they created a so-called 3D printed skin that was a flexible material that could be used for the sensor of the Tactip. These rigid tips act as pins that are printed onto flexible skin and serves as the active sensing surface. A

camera senses the movement of these pins depending upon the pressure that is applied. Because the sensing aspect and the holders can be printed it allows for complex features that would not normally be allowed to be created and accelerates the creation of new prototypes.[132]

Biomimetic phantoms can be used to replicate other vasculature systems, which can then be used for other types of measurements, like the amount of oxygenation in blood, as presented by Lv et al. To properly mimic the optical properties of the tissue, they mixed TiO_2 powder with the clear resin is to tune the refractive index and scattering properties of the phantom, in a similar fashion to Diep et al. Multispectral analysis is used to determine the oxygenation levels of blood in a retinal vascular phantom. This allows for a calibration curve to be made without the need of a patient.[133]

Along with phantoms, biomimetics allows for the creation of new optical structures based upon what is found in nature. Abid et al used angle-multiplexed optical printing to 3D-print an optical grating. The optical properties of these grating mimics that of a butterfly's wings and creates a distinct color because of the polarization of the grating, as shown in Figure 14.[18] Though the grating was implemented in a biomimetic fashion here, the ability to manufacture a custom grating in-house would be of great benefit for many laboratories.

Conclusion and Outlook

The development of 3D printing has been an impactful event for analytical chemistry, and science at large. The number of papers published using 3D printing has grown exponentially each year as this technology has allowed for rapid method development and democratized the fabrication of mechanical components. 3D printing has even allowed for better products to be made than were logistically possible before with previous methods like PDMS molding, as most prominently observed with microfluidics. There are still many opportunities for improvement, including improving feature resolution and surface roughness, as well as increasing structural strength so that sacrificial support materials are not needed. The capability and overall ease of use, however, has been more than enough to clearly make 3D printing one of the dominant next-generation fabrication and development techniques for advancing bioanalysis.

ACKNOWLEDGEMENTS

We would like to acknowledge the financial support from NSF (CHE-1413449) and NIH (R21AI140461).

VOCABULARY

3D Printing	Manufacturing method where two-dimensional layers or "slices" of an object are added sequentially according to a pre-determined pattern, building a total three-dimensional structure.
Optical Sensing	Analysis method of a given target where the collected signal is comprised of photons.

Rapid Prototyping	Design method where successive iterations of a new product can be easily modified and remade, speeding up the design process.
Microfluidics	The use of micrometer-scale channels and tubing through which to move fluid in order to drastically decrease the amount of fluid necessary for a given task.
Surface Plasmon	A propagating wave along a surface that extends perpendicularly out into the adjacent medium that is incited by absorbing incident light; changes in the light absorbance give information about the conditions on the surface.
Biomimetics	The manufacture of objects that resemble, in form or property, a biological structure.

REFERENCES

1. Xu YY; Wu XY; Guo X; Kong B; Zhang M; Qian X; Mi SL; Sun W, The Boom in 3D-Printed Sensor Technology. Sensors 2017, 17 (5), 1166.
2. Ambrosi A; Pumera M, 3D-printing technologies for electrochemical applications. Chem. Soc. Rev 2016, 45 (10), 2740–2755. [PubMed: 27048921]
3. Gross B; Lockwood SY; Spence DM, Recent Advances in Analytical Chemistry by 3D Printing. Analytical Chemistry 2017, 89 (1), 57–70. [PubMed: 28105825]
4. Kim P; Kwon KW; Park MC; Lee SH; Kim SM; Suh KY, Soft lithography for microfluidics: a review. BioChip J 2008, 2 (1), 1–11.
5. Au AK; Huynh W; Horowitz LF; Folch A, 3D-Printed Microfluidics. Angewandte Chemie-International Edition 2016, 55 (12), 3862–3881. [PubMed: 26854878]
6. Dirkzwager RM; Liang SL; Tanner JA, Development of Aptamer-Based Point-of-Care Diagnostic Devices for Malaria Using Three-Dimensional Printing Rapid Prototyping. Acs Sensors 2016, 1 (4), 420–426.
7. Macdonald NP; Currivan SA; Tedone L; Paull B, Direct Production of Microstructured Surfaces for Planar Chromatography Using 3D Printing. Analytical Chemistry 2017, 89 (4), 2457–2463. [PubMed: 28194964]
8. Chan HN; Tan MJA; Wu HK, Point-of-care testing: applications of 3D printing. Lab on a Chip 2017, 17 (16), 2713–2739. [PubMed: 28702608]
9. Hull CW Apparatus for production of three-dimensional objects by stereolithography US4575330 A, 3 11, 1986, 1986.
10. Cooke MN; Fisher JP; Dean D; Rimnac C; Mikos AG, Use of stereolithography to manufacture critical-sized 3D biodegradable scaffolds for bone ingrowth. J. Biomed. Mater. Res. Part B 2003, 64B (2), 65–69.
11. Bartolo PJ, Stereolithographic Processes In Stereolithography: Materials, Processes and Applications, Bartolo PJ, Ed. Springer: New York, USA, 2011; pp 1–36.
12. Tumbleston JR; Shirvanyants D; Ermoshkin N; Janusziewicz R; Johnson AR; Kelly D; Chen K; Pinschmidt R; Rolland JP; Ermoshkin A; Samulski ET; DeSimone JM, Continuous liquid interface production of 3D objects. Science 2015, 347 (6228), 1349–1352. [PubMed: 25780246]
13. Ostendorf A; Chichkov BN, Two-photon polymerization: A new approach to micromachining. Photonics Spectra 2006, 40 (10), 72–78.
14. Waheed S; Cabot JM; Macdonald NP; Lewis T; Guijt RM; Paull B; Breadmore MC, 3D printed microfluidic devices: enablers and barriers. Lab on a Chip 2016, 16 (11), 1993–2013. [PubMed: 27146365]

15. Ovsianikov A; Schlie S; Ngezahayo A; Haverich A; Chichkov BN, Two-photon polymerization technique for microfabrication of CAD-designed 3D scaffolds from commercially available photosensitive materials. J. Tissue Eng. Regen. Med 2007, 1 (6), 443–449. [PubMed: 18265416]
16. Patel DK; Sakhaei AH; Layani M; Zhang B; Ge Q; Magdassi S, Highly Stretchable and UV Curable Elastomers for Digital Light Processing Based 3D Printing. Advanced Materials 2017, 29 (15), 1606000.
17. Hong ZH; Liang RG, IR-laser assisted additive freeform optics manufacturing. Scientific Reports 2017, 7, 7145. [PubMed: 28769051]
18. Abid MI; Wang L; Chen QD; Wang XW; Juodkazis S; Sun HB, Angle-multiplexed optical printing of biomimetic hierarchical 3D textures. Laser Photon. Rev 2017, 11 (2), 1600187.
19. Gong H; Beauchamp M; Perry S; Woolley AT; Nordin GP, Optical approach to resin formulation for 3D printed microfluidics. Rsc Advances 2015, 5 (129), 106621–106632. [PubMed: 26744624]
20. Au AK; Bhattacharjee N; Horowitz LF; Chang TC; Folch A, 3D-printed microfluidic automation. Lab on a Chip 2015, 15 (8), 1934–1941. [PubMed: 25738695]
21. Crump SS Apparatus and method for creating three dimensional objects US5121329 A, 1992.
22. Waldbaur A; Rapp H; Lange K; Rapp BE, Let there be chip-towards rapid prototyping of microfluidic devices: one-step manufacturing processes. Analytical Methods 2011, 3 (12), 2681–2716.
23. Sood AK; Ohdar RK; Mahapatra SS, Parametric appraisal of mechanical property of fused deposition modelling processed parts. Mater. Des 2010, 31 (1), 287–295.
24. Zhong WH; Li F; Zhang ZG; Song LL; Li ZM, Short fiber reinforced composites for fused deposition modeling. Mater. Sci. Eng. A-Struct. Mater. Prop. Microstruct. Process 2001, 301 (2), 125–130.
25. Chia HN; Wu BM, Recent advances in 3D printing of biomaterials. J. Biol. Eng 2015, 9, 4. [PubMed: 25866560]
26. Li F; Smejkal P; Macdonald NP; Guijt RM; Breadmore MC, One-Step Fabrication of a Microfluidic Device with an Integrated Membrane and Embedded Reagents by Multimaterial 3D Printing. Analytical Chemistry 2017, 89 (8), 4701–4707. [PubMed: 28322552]
27. Feygin M Apparatus and method for forming an integral object from laminations US5354414 A, 1988.
28. Farahani RD; Dube M; Therriault D, Three-Dimensional Printing of Multifunctional Nanocomposites: Manufacturing Techniques and Applications. Advanced Materials 2016, 28 (28), 5794–5821. [PubMed: 27135923]
29. Gothait H Apparatus and method for three dimensional model printing US4938816 A, 2001.
30. Amin R; Knowlton S; Hart A; Yenilmez B; Ghaderinezhad F; Katebifar S; Messina M; Khademhosseini A; Tasoglu S, 3D-printed microfluidic devices. Biofabrication 2016, 8 (2), 022001–022017. [PubMed: 27321137]
31. Walczak R; Adamski K, Inkjet 3D printing of microfluidic structures-on the selection of the printer towards printing your own microfluidic chips. J. Micromech. Microeng 2015, 25 (8), 085013.
32. Top 4 Differences Between Stereolithography and PolyJet https://www.stratasysdirect.com (accessed June 5).
33. Begolo S; Zhukov DV; Selck DA; Li L; Ismagilov RF, The pumping lid: investigating multi-material 3D printing for equipment-free, programmable generation of positive and negative pressures for microfluidic applications. Lab on a Chip 2014, 14 (24), 4616–4628. [PubMed: 25231706]
34. Polyjet Materials: A Range of Possibilities http://web.stratasys.com/rs/objet/images/PolyJet%20materials%20white%20paper%20-%20English%20web.pdf (accessed August 4).
35. Beaman JJ Selective laser sintering with assisted powder handling US4938816 A, 1990.
36. Yazdi AA; Popma A; Wong W; Nguyen T; Pan YY; Xu J, 3D printing: an emerging tool for novel microfluidics and lab-on-a-chip applications. Microfluid. Nanofluid 2016, 20 (3), 50.
37. Vaezi M; Seitz H; Yang SF, A review on 3D micro-additive manufacturing technologies. Int. J. Adv. Manuf. Technol 2013, 67 (5-8), 1721–1754.

38. Capel AJ; Edmondson S; Christie SDR; Goodridge RD; Bibb RJ; Thurstans M, Design and additive manufacture for flow chemistry. Lab on a Chip 2013, 13 (23), 4583–4590. [PubMed: 24100659]
39. He Y; Yang FF; Zhao HM; Gao Q; Xia B; Fu JZ, Research on the printability of hydrogels in 3D bioprinting. Scientific Reports 2016, 6, 29977. [PubMed: 27436509]
40. Wang JP; Chiappone A; Roppolo I; Shao F; Fantino E; Lorusso M; Rentsch D; Dietliker K; Pirri CF; Grutzmacher H, All-in-One Cellulose Nanocrystals for 3D Printing of Nanocomposite Hydrogels. Angewandte Chemie-International Edition 2018, 57 (9), 2353–2356. [PubMed: 29266601]
41. Wu W; DeConinck A; Lewis JA, Omnidirectional Printing of 3D Microvascular Networks. Advanced Materials 2011, 23 (24), H178–H183. [PubMed: 21438034]
42. Santangelo MF; Libertino S; Turner APF; Filippini D; Mak WC, Integrating printed microfluidics with silicon photomultipliers for miniaturised and highly sensitive ATP bioluminescence detection. Biosensors & Bioelectronics 2018, 99, 464–470. [PubMed: 28820988]
43. Mattio E; Robert-Peillard F; Branger C; Puzio K; Margaillan A; Brach-Papa C; Knoery J; Boudenne JL; Coulomb B, 3D-printed flow system for determination of lead in natural waters. Talanta 2017, 168, 298–302. [PubMed: 28391857]
44. Gong H; Woolley AT; Nordin GP, High density 3D printed microfluidic valves, pumps, and multiplexers. Lab on a Chip 2016, 16 (13), 2450–2458. [PubMed: 27242064]
45. Rogers CI; Qaderi K; Woolley AT; Nordin GP, 3D printed microfluidic devices with integrated valves. Biomicrofluidics 2015, 9 (1), 016501. [PubMed: 25610517]
46. Donvito L; Galluccio L; Lombardo A; Morabito G; Nicolosi A; Reno M, Experimental validation of a simple, low-cost, T-junction droplet generator fabricated through 3D printing. J. Micromech. Microeng 2015, 25 (3), 035013.
47. Duarte LC; Chagas CLS; Ribeiro LEB; Coltro WKT, 3D printing of microfluidic devices with embedded sensing electrodes for generating and measuring the size of microdroplets based on contactless conductivity detection. Sensors and Actuators B-Chemical 2017, 251, 427–432.
48. Gelber MK; Kole MR; Kim N; Aluru NR; Bhargava R, Quantitative Chemical Imaging of Nonplanar Microfluidics. Analytical Chemistry 2017, 89 (3), 1716–1723. [PubMed: 27983804]
49. Macdonald NP; Cabot JM; Smejkal P; Guijt RM; Paull B; Breadmore MC, Comparing Microfluidic Performance of Three-Dimensional (3D) Printing Platforms. Analytical Chemistry 2017, 89 (7), 3858–3866. [PubMed: 28281349]
50. Li F; Macdonald NP; Guijt RM; Breadmore MC, Using Printing Orientation for Tuning Fluidic Behavior in Microfluidic Chips Made by Fused Deposition Modeling 3D Printing. Analytical Chemistry 2017, 89 (23), 12805–12811. [PubMed: 29048159]
51. Shallan AI; Smejkal P; Corban M; Guijt RM; Breadmore MC, Cost-Effective Three-Dimensional Printing of Visibly Transparent Microchips within Minutes. Analytical Chemistry 2014, 86 (6), 3124–3130. [PubMed: 24512498]
52. Chan HN; Shu YW; Xiong B; Chen YF; Chen Y; Tian Q; Michael SA; Shen B; Wu HK, Simple, Cost-Effective 3D Printed Microfluidic Components for Disposable, Point-of-Care Colorimetric Analysis. Acs Sensors 2016, 1 (3), 227–234.
53. Hampson SM; Rowe W; Christie SDR; Platt M, 3D printed microfluidic device with integrated optical sensing for particle analysis. Sensors and Actuators B-Chemical 2018, 256, 1030–1037.
54. Tang CK; Vaze A; Rusling JF, Automated 3D-printed unibody immunoarray for chemiluminescence detection of cancer biomarker proteins. Lab on a Chip 2017, 17 (3), 484–489. [PubMed: 28067370]
55. Kadimisetty K; Mosa IM; Malla S; Satterwhite-Warden JE; Kuhns TM; Faria RC; Lee NH; Rusling JF, 3D-printed supercapacitor-powered electrochemiluminescent protein immunoarray. Biosensors & Bioelectronics 2016, 77, 188–193. [PubMed: 26406460]
56. Kadimisetty K; Malla S; Bhalerao KS; Mosa IM; Bhakta S; Lee NH; Rusling JF, Automated 3D-Printed Microfluidic Array for Rapid Nanomaterial-Enhanced Detection of Multiple Proteins. Analytical Chemistry 2018, 90 (12), 7569–7577. [PubMed: 29779368]

57. Kadimisetty K; Malla S; Rusling JF, Automated 3-D Printed Arrays to Evaluate Genotoxic Chemistry: E-Cigarettes and Water Samples. Acs Sensors 2017, 2 (5), 670–678. [PubMed: 28723166]
58. Bauer M; Kulinsky L, Fabrication of a Lab-on-Chip Device Using Material Extrusion (3D Printing) and Demonstration via Malaria-Ab ELISA. Micromachines 2018, 9 (1), 27.
59. Roda A; Michelini E; Cevenini L; Calabria D; Calabretta MM; Simoni P, Integrating Biochemiluminescence Detection on Smartphones: Mobile Chemistry Platform for Point-of-Need Analysis. Analytical Chemistry 2014, 86 (15), 7299–7304. [PubMed: 25017302]
60. Ko J; Hemphill MA; Gabrieli D; Wu L; Yelleswarapu V; Lawrence G; Pennycooke W; Singh A; Meaney DF; Issadore D, Smartphone-enabled optofluidic exosome diagnostic for concussion recovery. Scientific Reports 2016, 6, 31215. [PubMed: 27498963]
61. Liu CC; Liao SC; Song JZ; Mauk MG; Li XW; Wu GX; Ge DT; Greenberg RM; Yang S; Bau HH, A high-efficiency superhydrophobic plasma separator. Lab on a Chip 2016, 16 (3), 553–560. [PubMed: 26732765]
62. Lee W; Kwon D; Choi W; Jung GY; Jeon S, 3D-Printed Microfluidic Device for the Detection of Pathogenic Bacteria Using Size-based Separation in Helical Channel with Trapezoid Cross-Section. Scientific Reports 2015, 5, 7717. [PubMed: 25578942]
63. Park C; Lee J; Kim Y; Kim J; Park S, 3D-printed microfluidic magnetic preconcentrator for the detection of bacterial pathogen using an ATP luminometer and antibody-conjugated magnetic nanoparticles. Journal of Microbiological Methods 2017, 132, 128–133. [PubMed: 27923650]
64. Ganesh I; Tran BM; Kim Y; Kim J; Cheng H; Lee NY; Park S, An integrated microfluidic PCR system with immunomagnetic nanoparticles for the detection of bacterial pathogens. Biomedical Microdevices 2016, 18 (6), 116. [PubMed: 27975186]
65. Han N; Shin JH; Han KH, An on-chip RT-PCR microfluidic device, that integrates mRNA extraction, cDNA synthesis, and gene amplification. Rsc Advances 2014, 4 (18), 9160–9165.
66. Kataoka EM; Murer RC; Santos JM; Carvalho RM; Eberlin MN; Augusto F; Poppi RJ; Gobbi AL; Hantao LW, Simple, Expendable, 3D-Printed Microfluidic Systems for Sample Preparation of Petroleum. Analytical Chemistry 2017, 89 (6), 3460–3467. [PubMed: 28230979]
67. Calderilla C; Maya F; Cerda V; Leal LO, 3D printed device including disk-based solid-phase extraction for the automated speciation of iron using the multisyringe flow injection analysis technique. Talanta 2017, 175, 463–469. [PubMed: 28842018]
68. Calderilla C; Maya F; Cerda V; Leal LO, 3D printed device for the automated preconcentration and determination of chromium (VI). Talanta 2018, 184, 15–22. [PubMed: 29674027]
69. Su CK; Peng PJ; Sun YC, Fully 3D-Printed Preconcentrator for Selective Extraction of Trace Elements in Seawater. Analytical Chemistry 2015, 87 (13), 6945–6950. [PubMed: 26101898]
70. Belka M; Ulenberg S; Baczek T, Fused Deposition Modeling Enables the Low-Cost Fabrication of Porous, Customized-Shape Sorbents for Small-Molecule Extraction. Analytical Chemistry 2017, 89 (8), 4373–4376. [PubMed: 28361532]
71. Fichou D; Morlock GE, Open-Source-Based 3D Printing of Thin Silica Gel Layers in Planar Chromatography. Analytical Chemistry 2017, 89 (3), 2116–2122. [PubMed: 28208299]
72. Gross BC; Anderson KB; Meisel JE; McNitt MI; Spence DM, Polymer Coatings in 3D-Printed Fluidic Device Channels for Improved Cellular Adherence Prior to Electrical Lysis. Analytical Chemistry 2015, 87 (12), 6335–6341. [PubMed: 25973637]
73. Paknahad M; Bachhal JS; Ahmadi A; Hoorfar M, Characterization of channel coating and dimensions of microfluidic-based gas detectors. Sensors and Actuators B-Chemical 2017, 241, 55–64.
74. Ohtani K; Tsuchiya M; Sugiyama H; Katakura T; Hayakawa M; Kanai T, Surface Treatment of Flow Channels in Microfluidic Devices Fabricated by Stereolithography. J. Oleo Sci 2014, 63 (1), 93–96. [PubMed: 24389798]
75. Song SY; Park MS; Lee JW; Yun JS, A Study on the Rheological and Mechanical Properties of Photo-Curable Ceramic/Polymer Composites with Different Silane Coupling Agents for SLA 3D Printing Technology. Nanomaterials 2018, 8 (2), 93.
76. Ligon-Auer SC; Schwentenwein M; Gorsche C; Stampfl J; Liska R, Toughening of photo-curable polymer networks: a review. Polym. Chem 2016, 7 (2), 257–286.

77. Matsumoto I; Seno N; Golovtchenkomatsumoto AM; Osawa T, AMINATION AND SUBSEQUENT DERIVATIZATION OF EPOXY-ACTIVATED AGAROSE FOR THE PREPARATION OF NEW AFFINITY ADSORBENTS. Journal of Biochemistry 1980, 87 (2), 535–540. [PubMed: 7358652]

78. Credi C; Griffini G; Levi M; Turri S, Biotinylated Photopolymers for 3D-Printed Unibody Lab-on-a-Chip Optical Platforms. Small 2018, 14 (1), 1702831.

79. Wang LJ; Chang YC; Sun RR; Li L, A multichannel smartphone optical biosensor for high-throughput point-of-care diagnostics. Biosensors & Bioelectronics 2017, 87, 686–692. [PubMed: 27631683]

80. Chan HN; Chen YF; Shu YW; Chen Y; Tian Q; Wu HK, Direct, one-step molding of 3D-printed structures for convenient fabrication of truly 3D PDMS microfluidic chips. Microfluid. Nanofluid 2015, 19 (1), 9–18.

81. Whitesides GM; Tang SKY In Fluidic optics, Conference on Optofluidics, San Diego, CA, Aug 15-16; Harvard Univ, D. C.; Chem Biol, O. S. C. M. A. U. S. A., Eds. Spie-Int Soc Optical Engineering: San Diego, CA, 2006.

82. Zhu F; Macdonald NP; Cooper JM; Wlodkowic D In Additive manufacturing of Lab-on-a-Chip devices: Promises and Challenges, Conference on Micro/Nano Materials, Devices, and Systems, Melbourne, AUSTRALIA, Dec 09-11; Rmit Univ, S. A. S. O. F. M. V. A.; Univ Glasgow, S. E. G. G. Q. Q. L. S., Eds. Spie-Int Soc Optical Engineering: Melbourne, AUSTRALIA, 2013.

83. Debellemaniere G; Flores M; Montard M; Delbosc B; Saleh M, Three-dimensional Printing of Optical Lenses and Ophthalmic Surgery: Challenges and Perspectives. J. Refractive Surg 2016, 32 (3), 201–204.

84. Gawedzinski J; Pawlowski ME; Tkaczyk TS, Quantitative evaluation of performance of three-dimensional printed lenses. Opt. Eng 2017, 56 (8), 084110. [PubMed: 29238114]

85. Gissibl T; Thiele S; Herkommer A; Giessen H, Two-photon direct laser writing of ultracompact multi-lens objectives. Nature Photonics 2016, 10 (8), 554–560.

86. Dietrich PI; Blaicher M; Reuter I; Billah M; Hoose T; Hofmann A; Caer C; Dangel R; Offrein B; Troppenz U; Moehrle M; Freude W; Koos C, In situ 3D nanoprinting of free-form coupling elements for hybrid photonic integration. Nature Photonics 2018, 12 (4), 241–247.

87. Peng WJ; Hsu WY; Cheng YC; Lin WL; Yu ZR; Chou HY; Chen FZ; Fu CC; Wu CS; Huang CT In Multiple-aperture optical design for micro-level cameras using 3D-printing method, Conference on Photonic Instrumentation Engineering V, San Francisco, CA, Jan 30-Feb 01; San Francisco, CA, 2018.

88. Sugioka K; Cheng Y, Femtosecond laser three-dimensional micro- and nanofabrication. Appl. Phys. Rev 2014, 1 (4), 041303.

89. Comina G; Suska A; Filippini D, Autonomous Chemical Sensing Interface for Universal Cell Phone Readout. Angewandte Chemie-International Edition 2015, 54 (30), 8708–8712. [PubMed: 26095136]

90. Comina G; Suska A; Filippini D, A 3D printed device for quantitative enzymatic detection using cell phones. Analytical Methods 2016, 8 (32), 6135–6142.

91. Vaidya N; Solgaard O, 3D printed optics with nanometer scale surface roughness. Microsyst. Nanoeng 2018, 4, 18.

92. Hinman SS; McKeating KS; Cheng Q, Plasmonic Sensing with 3D Printed Optics. Analytical Chemistry 2017, 89 (23), 12626–12630. [PubMed: 29156138]

93. Dewey MP; Ulutan D; Asme, DEVELOPMENT OF LASER POLISHING AS AN AUXILIARY POST-PROCESS TO IMPROVE SURFACE QUALITY IN FUSED DEPOSITION MODELING PARTS Proceedings of the Asme 12th International Manufacturing Science and Engineering Conference - 2017, Vol 2 2017, 6.

94. Li JW; Nallappan K; Guerboukha H; Skorobogatiy M, 3D printed hollow core terahertz Bragg waveguides with defect layers for surface sensing applications. Optics Express 2017, 25 (4), 4126–4144. [PubMed: 28241619]

95. Pandey S; Gupta B; Nahata A, Terahertz plasmonic waveguides created via 3D printing. Optics Express 2013, 21 (21), 24422–24430. [PubMed: 24150287]

96. Squires AD; Constable E; Lewis RA, 3D Printed Terahertz Diffraction Gratings And Lenses. Journal of Infrared Millimeter and Terahertz Waves 2015, 36 (1), 72–80.

97. Busch SF; Castro-Camus E; Beltran-Mejia F; Balzer JC; Koch M, 3D Printed Prisms with Tunable Dispersion for the THz Frequency Range. Journal of Infrared Millimeter and Terahertz Waves 2018, 39 (6), 553–560.

98. Busch SF; Weidenbach M; Fey M; Schafer F; Probst T; Koch M, Optical Properties of 3D Printable Plastics in the THz Regime and their Application for 3D Printed THz Optics. Journal of Infrared Millimeter and Terahertz Waves 2014, 35 (12), 993–997.

99. Weber MJ, Handbook of optical materials CRC Press: 2002.

100. Klein J; Stern M; Franchin G; Kayser M; Inamura C; Dave S; Weaver JC; Houk P; Colombo P; Yang M; Oxman N, Additive Manufacturing of Optically Transparent Glass. 3D Print. Addit. Manuf 2015, 2 (3), 92–105.

101. Bergmann C; Lindner M; Zhang W; Koczur K; Kirsten A; Telle R; Fischer H, 3D printing of bone substitute implants using calcium phosphate and bioactive glasses. J. Eur. Ceram. Soc 2010, 30 (12), 2563–2567.

102. Fu QA; Saiz E; Tomsia AP, Bioinspired Strong and Highly Porous Glass Scaffolds. Adv. Funct. Mater 2011, 21 (6), 1058–1063. [PubMed: 21544222]

103. Kotz F; Arnold K; Bauer W; Schild D; Keller N; Sachsenheimer K; Nargang TM; Richter C; Helmer D; Rapp BE, Three-dimensional printing of transparent fused silica glass. Nature 2017, 544 (7650), 337–339. [PubMed: 28425999]

104. Cooperstein I; Shukrun E; Press O; Kamyshny A; Magdassi S, Additive Manufacturing of Transparent Silica Glass from Solutions. Acs Applied Materials & Interfaces 2018, 10 (22), 18879–18885. [PubMed: 29741081]

105. Destino JF; Dudukovic NA; Johnson MA; Nguyen DT; Yee TD; Egan GC; Sawvel AM; Steele WA; Baumann TF; Duoss EB; Suratwala T; Dylla-Spears R, 3D Printed Optical Quality Silica and Silica-Titania Glasses from Sol-Gel Feedstocks. Adv. Mater. Technol 2018, 3 (6), 1700323.

106. Nguyen DT; Meyers C; Yee TD; Dudukovic NA; Destino JF; Zhu C; Duoss EB; Baumann TF; Suratwala T; Smay JE; Dylla-Spears R, 3D-Printed Transparent Glass. Advanced Materials 2017, 29 (26), 1701181.

107. Luo JJ; Gilbert LJ; Qu C; Landers RG; Bristow DA; Kinzel EC, Additive Manufacturing of Transparent Soda-Lime Glass Using a Filament-Fed Process. J. Manuf. Sci. Eng.-Trans. ASME 2017, 139 (6), 061006.

108. Luo JJ; Gilbert LJ; Bristow DA; Landers RG; Goldstein JT; Urbas AM; Kinzel EC In Additive manufacturing of glass for optical applications, Conference on Laser 3D Manufacturing III, San Francisco, CA, Feb 15-18; Missouri Univ, S.; Technol, M.; Aerosp Engn, W. t. S. R. M. O. U. S. A.; Air Force Res Lab, M.; Mfg Directorate, W. P. A. F. B. O. H. U. S. A., Eds. Spie-Int Soc Optical Engineering: San Francisco, CA, 2016; p 061006.

109. Kooyman R, P H, Physics of Surface Plasmon Resonance In Handbook of Surface Plasmon Resonance, Schasfoort RBM, Ed. Royal Society of Chemistry: Cambridge, UK, 2008; pp 15–34.

110. Haring AP; Khan AU; Liu GL; Johnson BN, 3D Printed Functionally Graded Plasmonic Constructs. Adv. Opt. Mater 2017, 5 (18), 1700367.

111. Homola J; Yee SS; Gauglitz G, Surface plasmon resonance sensors: review. Sensors and Actuators B-Chemical 1999, 54 (1-2), 3–15.

112. Hwang Y; Gupta NK; Ojha YR; Cameron BD In An optical sensing approach for the noninvasive transdermal monitoring of cortisol, Conference on Nanoscale Imaging, Sensing, and Actuation for Biomedical Applications XIII, San Francisco, CA, Feb 15-17; Univ Toledo, D. B. N. H. M. S. W. B. S. T. O. H. U. S. A., Ed. Spie-Int Soc Optical Engineering: San Francisco, CA, 2016.

113. Zhang CG; Chen CJ; Settu K; Liu JT, Angle-Scanning Surface Plasmon Resonance System with 3D Printed Components for Biorecognition Investigation. Adv. Condens. Matter Phys 2018, 5654010.

114. Guner H; Ozgur E; Kokturk G; Celik M; Esen E; Topal AE; Ayas S; Uludag Y; Elbuken C; Dana A, A smartphone based surface plasmon resonance imaging (SPRi) platform for on-site biodetection. Sensors and Actuators B-Chemical 2017, 239, 571–577.

115. Herzog D; Seyda V; Wycisk E; Emmelmann C, Additive manufacturing of metals. Acta Mater 2016, 117, 371–392.
116. Randolph SJ; Fowlkes JD; Rack PD, Focused, nanoscale electron-beam-induced deposition and etching. Crit. Rev. Solid State Mat. Sci 2006, 31 (3), 55–89.
117. Winkler R; Schrnidt FP; Haselinann U; Fowlkes JD; Lewis BB; Kothleitner G; Rack PD; Plank H, Direct-Write 3D Nanoprinting of Plasmonic Structures. Acs Applied Materials & Interfaces 2017, 9 (9), 8233–8240. [PubMed: 28269990]
118. Lee E; Seo IC; Jeong HY; An SC; Jun YC, Theoretical investigations on microwave Fano resonances in 3D-printable hollow dielectric resonators. Scientific Reports 2017, 7, 16186. [PubMed: 29170527]
119. Gupta MK; Meng F; Johnson BN; Kong YL; Tian LM; Yeh YW; Masters N; Singamaneni S; McAlpine MC, 3D Printed Programmable Release Capsules. Nano Lett 2015, 15 (8), 5321–5329. [PubMed: 26042472]
120. Wang YJ; Zeinhom MMA; Yang MM; Sun RR; Wang SF; Smith JN; Timchalk C; Li L; Lin YH; Du D, A 3D-Printed, Portable, Optical-Sensing Platform for Smartphones Capable of Detecting the Herbicide 2,4-Dichlorophenoxyacetic Acid. Analytical Chemistry 2017, 89 (17), 9339–9346. [PubMed: 28727917]
121. Cevenini L; Calabretta MM; Tarantino G; Michelini E; Roda A, Smartphone-interfaced 3D printed toxicity biosensor integrating bioluminescent “sentinel cells”. Sensors and Actuators B-Chemical 2016, 225, 249–257.
122. Javidi B; Markman A; Rawat S; O’Connor T; Anand A; Andemariam B, Sickle cell disease diagnosis based on spatio-temporal cell dynamics analysis using 3D printed shearing digital holographic microscopy. Optics Express 2018, 26 (10), 13614–13627. [PubMed: 29801384]
123. Pandey V; Gupta S; Elangovan R, Compact 3D printed module for fluorescence and label-free imaging using evanescent excitation. Methods and Applications in Fluorescence 2018, 6 (1), 015007.
124. Schafer M; Brauler V; Ulber R, Bio-sensing of metal ions by a novel 3D-printable smartphone spectrometer. Sensors and Actuators B-Chemical 2018, 255, 1902–1910.
125. Bayram A; Serhatlioglu M; Ortac B; Demic S; Elbuken C; Sen M; Solmaz ME, Integration of glass micropipettes with a 3D printed aligner for microfluidic flow cytometer. Sensors and Actuators a-Physical 2018, 269, 382–387.
126. van den Driesche S; Lucklum F; Bunge F; Vellekoop MJ, 3D Printing Solutions for Microfluidic Chip-To-World Connections. Micromachines 2018, 9 (2), 71.
127. Mendoza-Gallegos RA; Rios A; Garcia-Cordero JL, An Affordable and Portable Thermocycler for Real-Time PCR Made of 3D-Printed Parts and Off-the-Shelf Electronics. Analytical Chemistry 2018, 90 (9), 5563–5568. [PubMed: 29624373]
128. Liu Y; Ghassemi P; Depkon A; Iacono MI; Lin J; Mendoza G; Wang JT; Tang QG; Chen Y; Pfefer TJ, Biomimetic 3D-printed neurovascular phantoms for near-infrared fluorescence imaging. Biomedical Optics Express 2018, 9 (6), 2810–2824. [PubMed: 30258692]
129. Bentz BZ; Bowen AG; Lin D; Ysselstein D; Huston DH; Rochet JC; Webb KJ, Printed optics: phantoms for quantitative deep tissue fluorescence imaging. Opt. Lett 2016, 41 (22), 5230–5233. [PubMed: 27842100]
130. Dempsey LA; Persad M; Powell S; Chitnis D; Hebden JC, Geometrically complex 3D-printed phantoms for diffuse optical imaging. Biomedical Optics Express 2017, 8 (3), 1754–1762. [PubMed: 28663863]
131. Diep P; Pannem S; Sweer J; Lo J; Snyder M; Stueber G; Zhao YY; Tabassum S; Istfan R; Wu JJ; Erramilli S; Roblyer D, Three-dimensional printed optical phantoms with customized absorption and scattering properties. Biomedical Optics Express 2015, 6 (11), 4212–4220. [PubMed: 26600987]
132. Ward-Cherrier B; Pestell N; Cramphorn L; Winstone B; Giannaccini ME; Rossiter J; Lepora NF, The TacTip Family: Soft Optical Tactile Sensors with 3D-Printed Biomimetic Morphologies. Soft Robotics 2018, 5 (2), 216–227. [PubMed: 29297773]

133. Lv X; Chen HY; Liu GL; Shen SW; Wu Q; Hu CZ; Li JL; Dong EB; Xu RX, Design of a portable phantom device to simulate tissue oxygenation and blood perfusion. Applied Optics 2018, 57 (14), 3938–3946. [PubMed: 29791363]

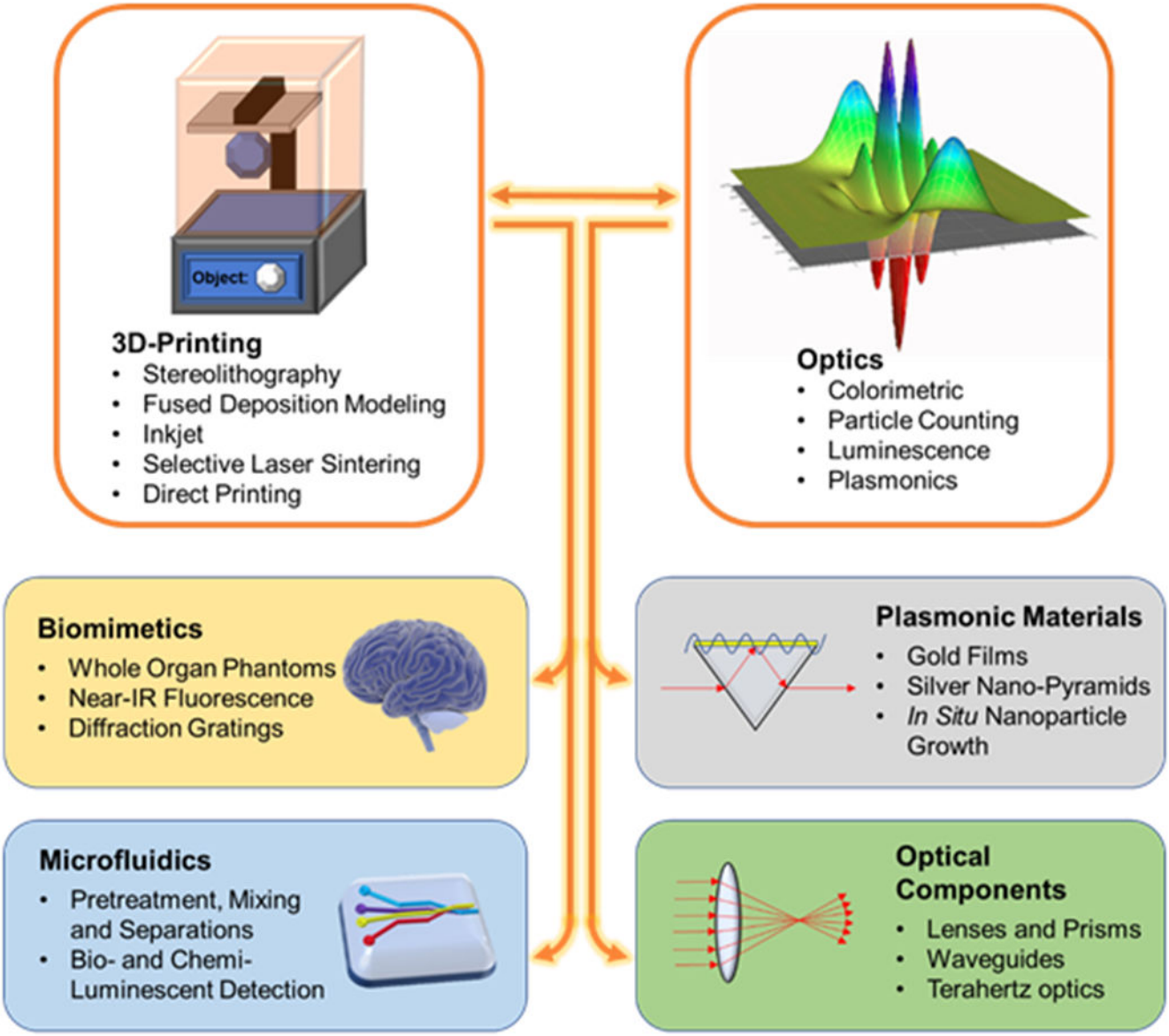

Figure 1.

3D-Printing enables a wide range of applications for optical sensors. 3D-printing's ability to prototype new designs effectively is effectively combined with a range of optical techniques.

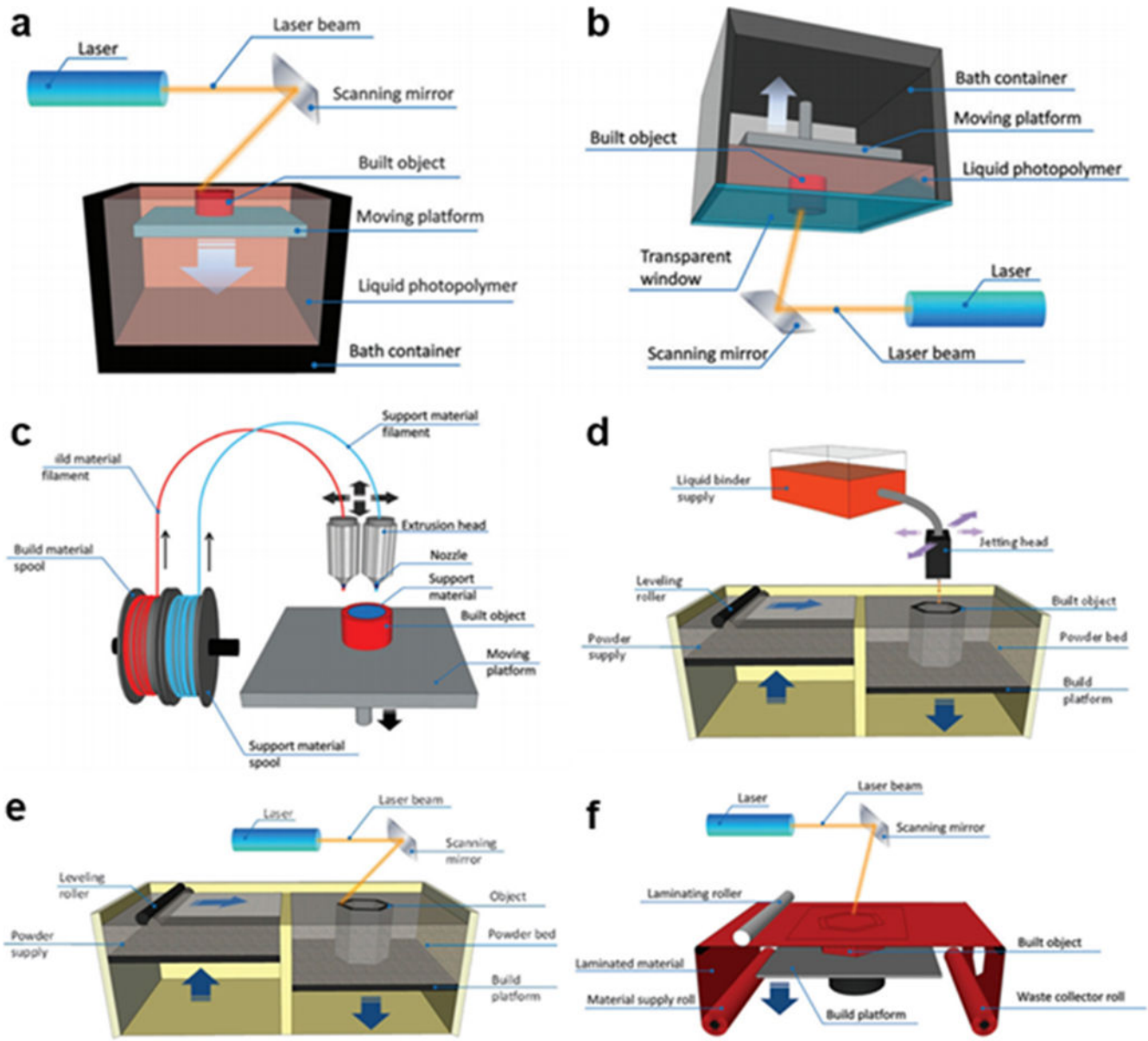

Figure 2.

Functional schemes of 3D printing technologies: (a) SLA, bath configuration; (b) SLA, bat configuration; (c) FDM; (d) Inkjet; (e) SLS; (f) LOM (Reprinted with permission from ref 2 Copyright 2016 Royal Society of Chemistry).

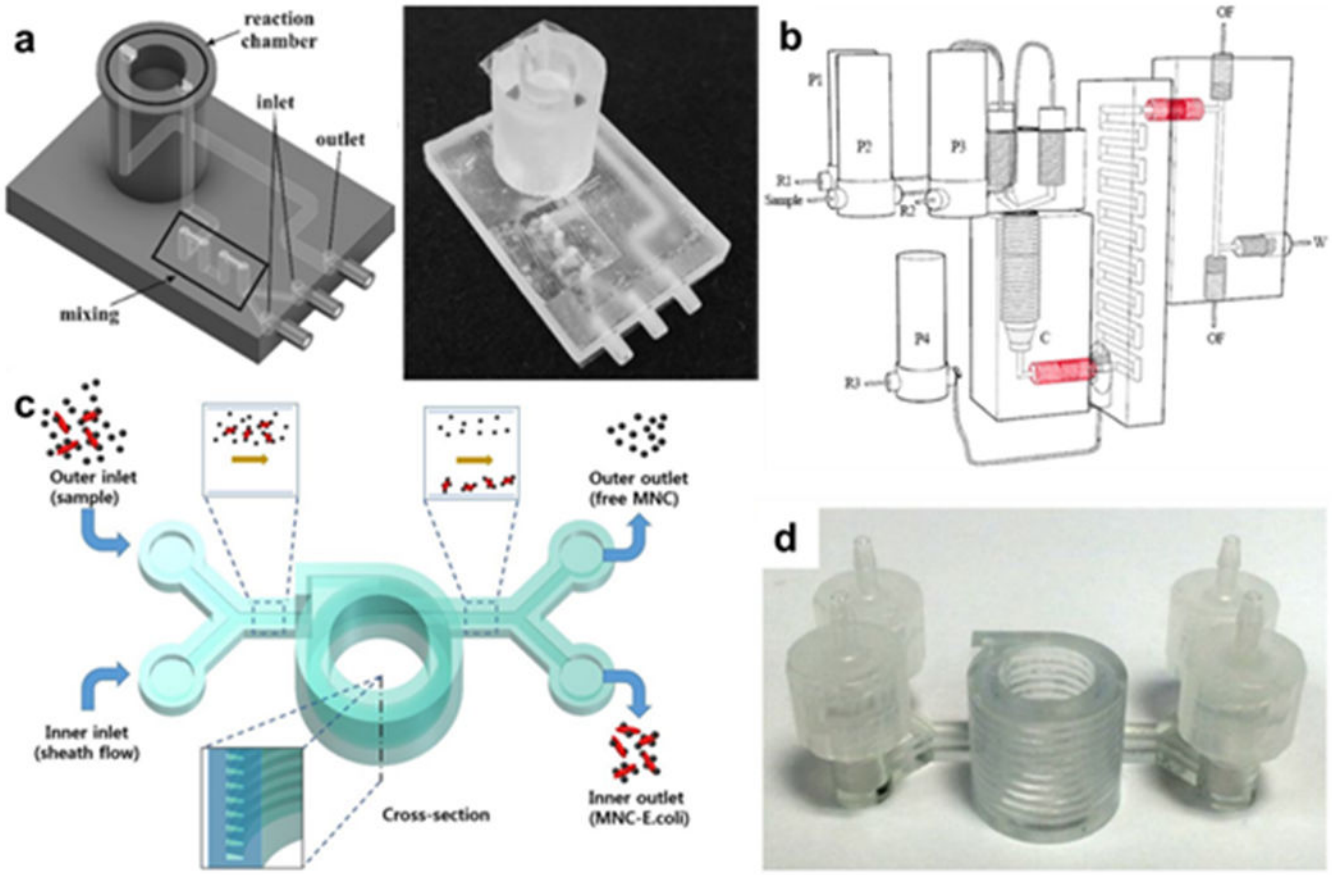

Figure 3.

3D-printed microfluidic architectures. (a) Left: Schematic of ATP monitoring device that uses a luciferase reaction, where dual inlets are mixed and then detected in the reaction chamber. Right: photograph of actual SLA-printed device (Reprinted with permission from ref 42 Copyright 2018 Elsevier). (b) Schematic of 3D architecture that adds a second reagent after a preconcentration step (Reprinted with permission from ref 43 Copyright 2017 Elsevier). (c) Helical 3D-printed separation chamber and (d) the corresponding actual object (Reprinted with permission from ref 62 Copyright 2017 Springer).

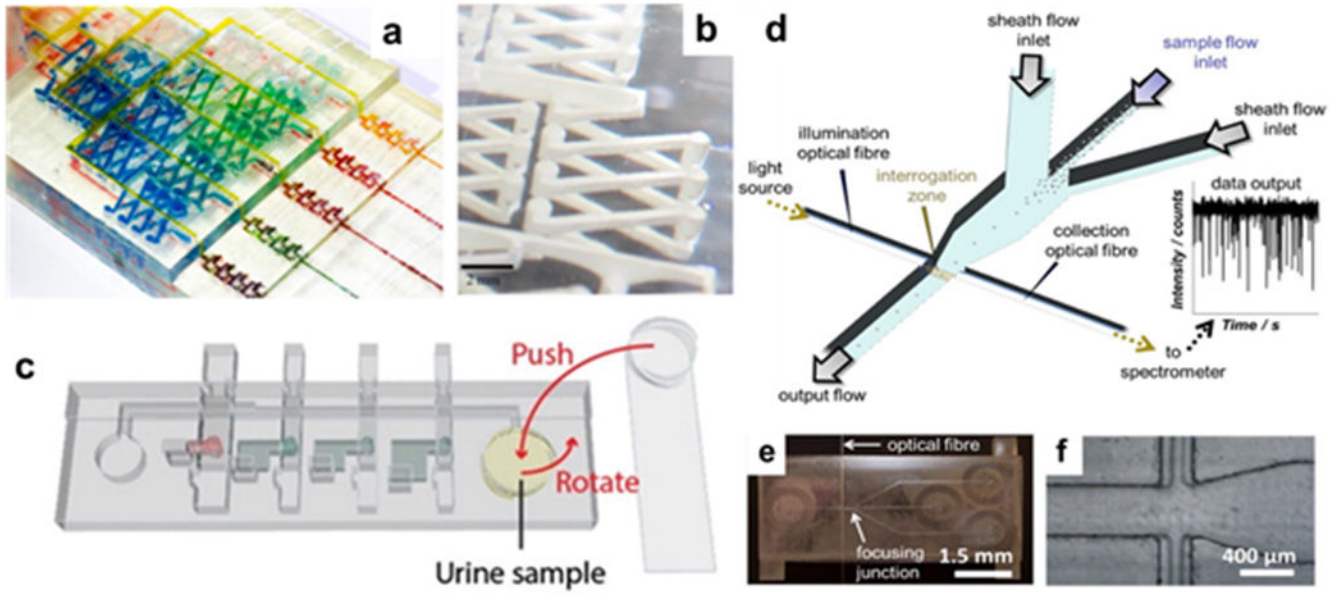

Figure 4.

3D-printed optical detection devices. (a) Colorimetric detection via Griess test, where each channel is a point in a standard addition curve, and (b) close-up of the mixing channel (Reprinted with permission from ref 51 Copyright 2014 American Chemical Society). (c) Integrated printed unit for colorimetric sensing with manual rotary pump and multiple valves for reagent reservoirs (Reprinted with permission from ref 52 Copyright 2016 American Chemical Society). (d) Schematic for sheath flow focusing apparatus for optical particle detection, and (e) images of actual device and (f) focusing junction (Reprinted with permission from ref 53 Copyright 2018 Elsevier).

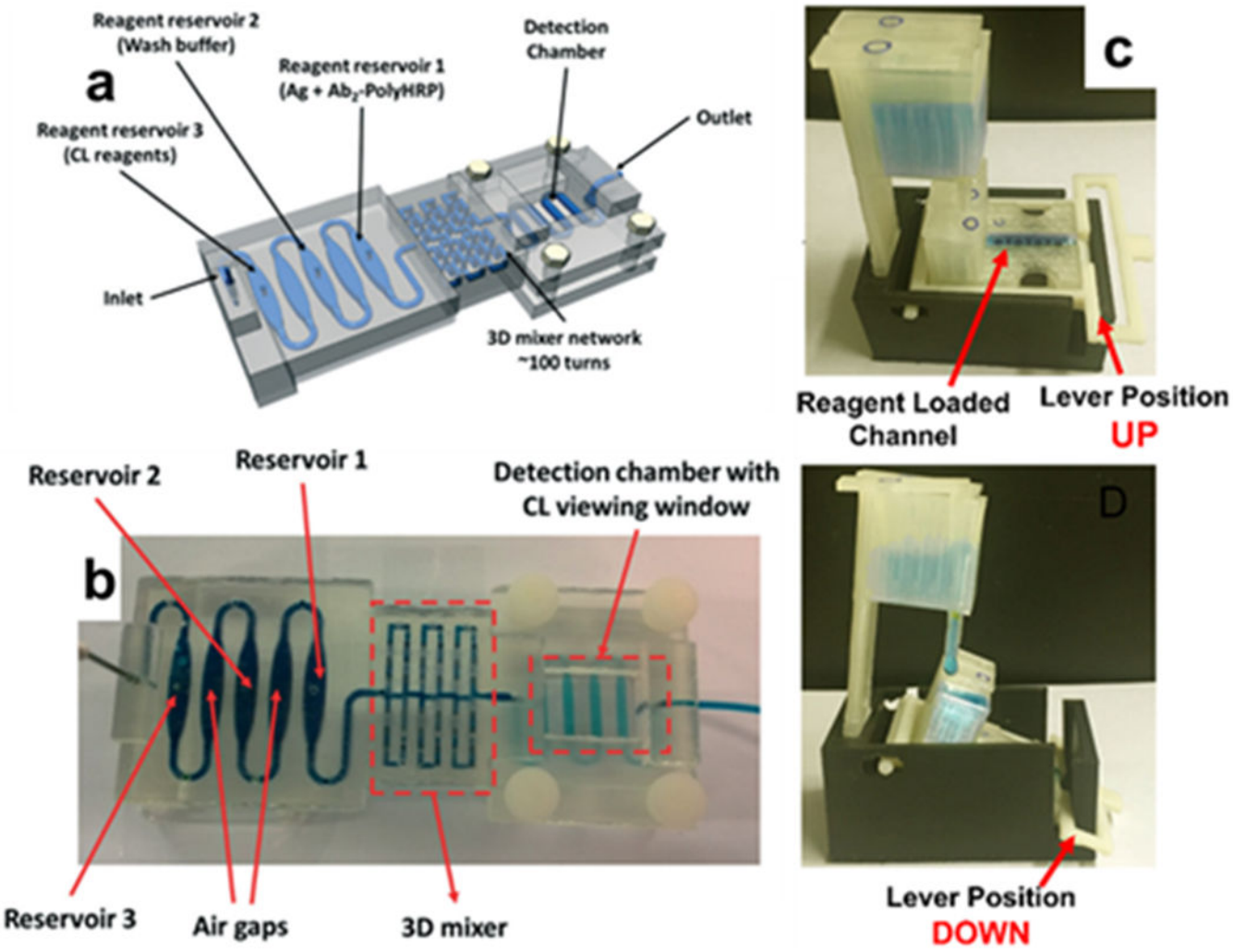

Figure 5.

3D-printed detectors based on luminescence. (a) Schematic and (b) printed device of unibody chemiluminescent detector (Reprinted with permission from ref 54 Copyright 2017 Royal Society of Chemistry). (c) 3D-printed module with two configurations: “up” (top), where multiple reservoirs that dispenses reagents into the lower chamber; and “down” (bottom), where the reagents wash down to the electrode array below for electrochemiluminescent detection (Reprinted with permission from ref 55 Copyright 2016 Elsevier).

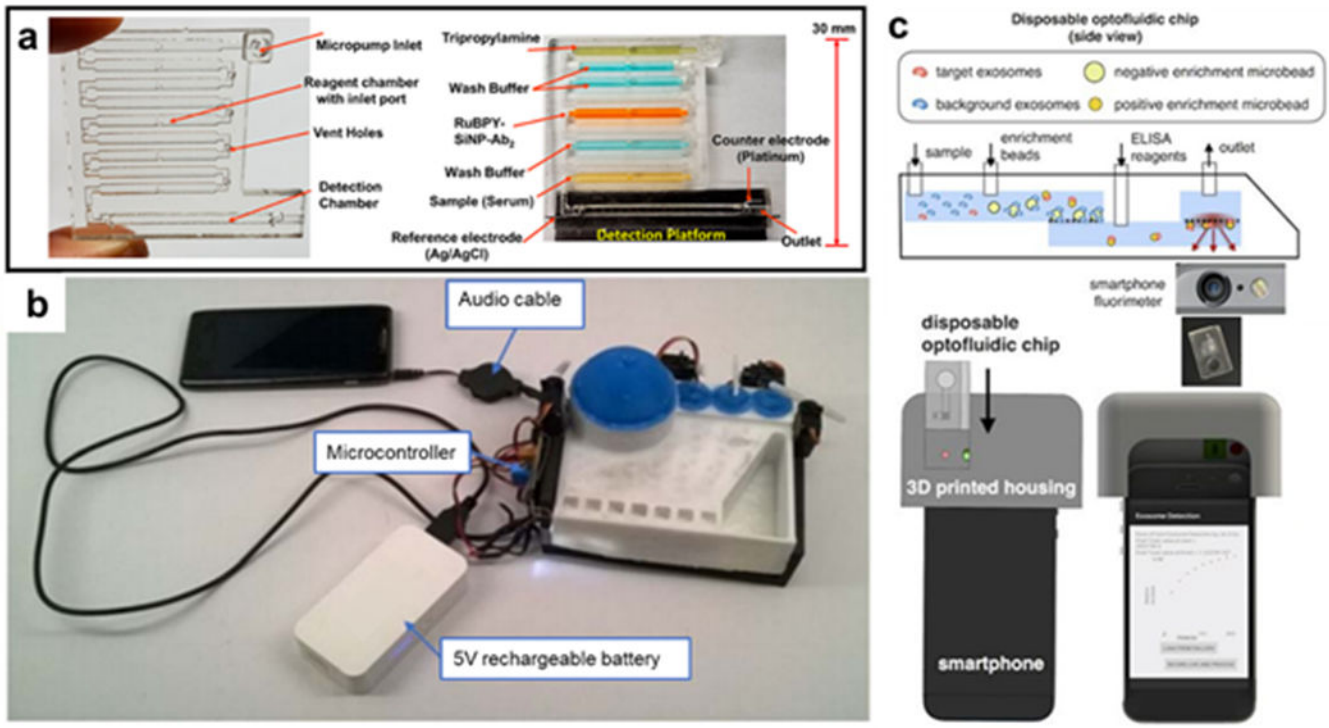

Figure 6.

Electronics-integrated 3D-printed analysis devices. (a) Automated ECL array for multiplexed detection with 3D-printed flow cell (Reprinted with permission from ref 56 Copyright 2018 American Chemical Society) (b) Example microfluidic module integrated with a flexible system of electronic pump/actuators that are controlled by a “song” file on an audio device (from ref 58) (c) Smartphone accessory utilizing microfluidic isolation of concussion-linked exosomes for ELISA detection using the smartphone camera (Reprinted with permission from ref 60 Copyright 2016 Springer).

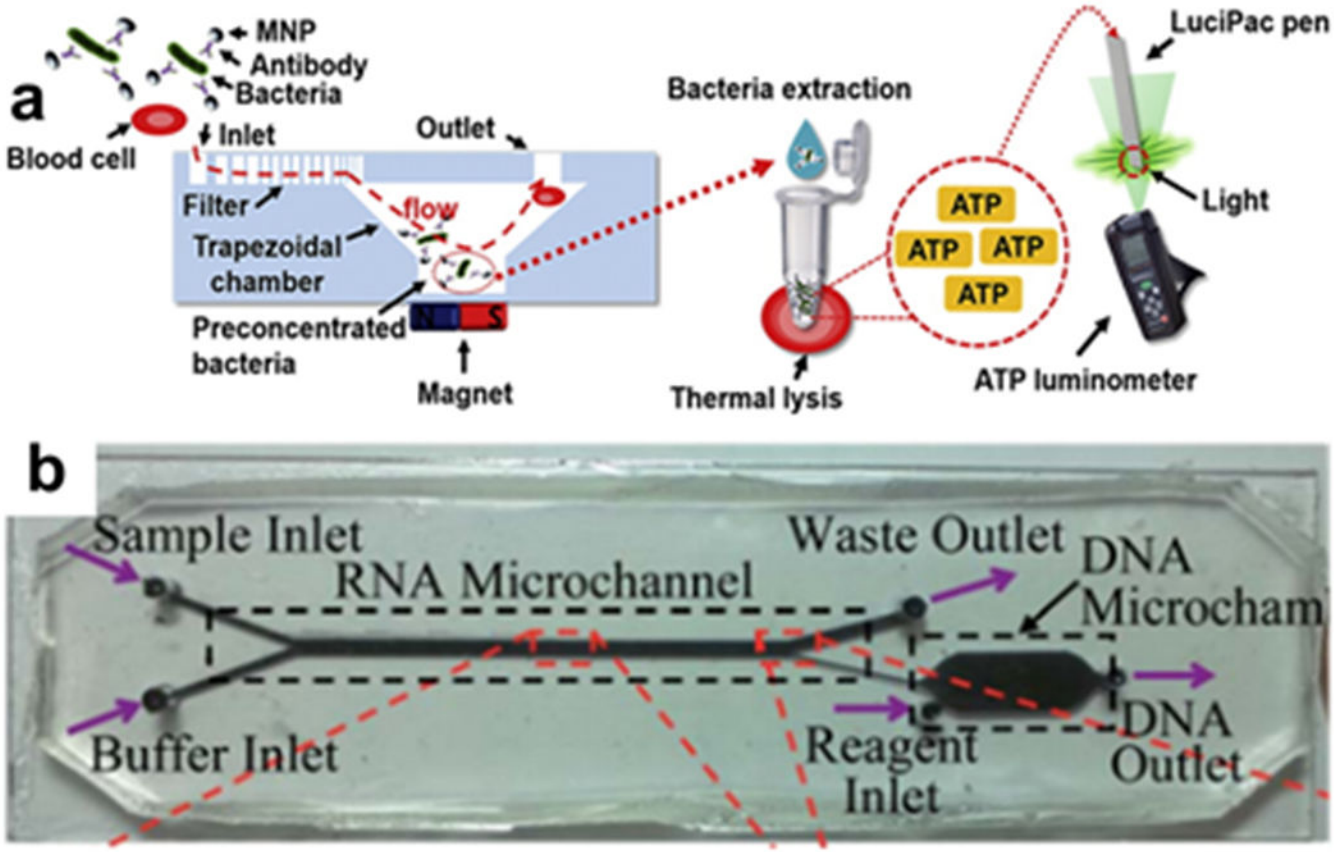

Figure 7.

3D-printed preconcentrators. (a) A conical concentration chamber separates MNP-functionalized from blood, followed by ATP luminescence detection. (Reprinted with permission from ref 63 Copyright 2017 Elsevier) (b) The magnetic chamber here separates MNP-functionalized RNA into a secondary chamber for cDNA synthesis and PCR (Reprinted with permission from ref 65 Copyright 2014 Royal Society of Chemistry).

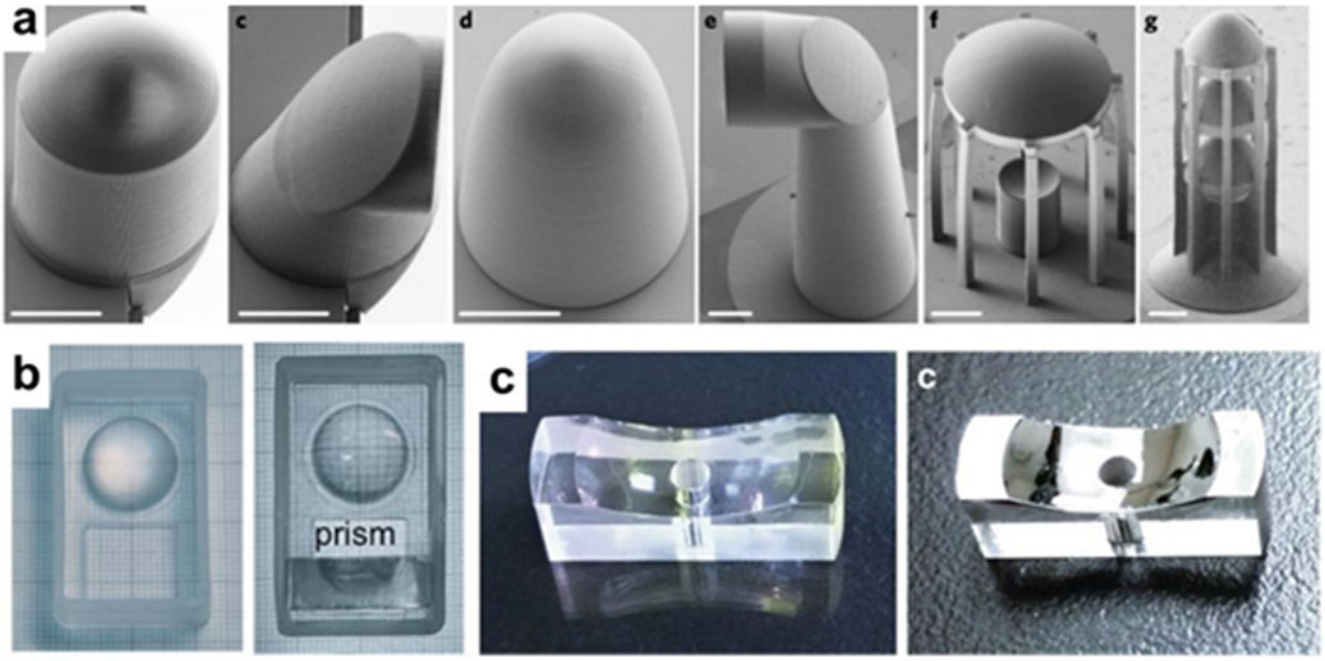

Figure 8.

3D-printed optics. (a) Microstructured free-form coupling elements fabricated with two-photon polymerization (Reprinted with permission from ref 86 Copyright 2018 Springer). (b) Prism and lens assembly before (left) and after (right) post-processing resin coating step (Reprinted with permission from ref 90 Copyright 2016 Royal Society of Chemistry). (c) Printed and resin-coated mirror before (left) and after (right) metallization (Reprinted with permission from ref 91 Copyright 2018 Springer).

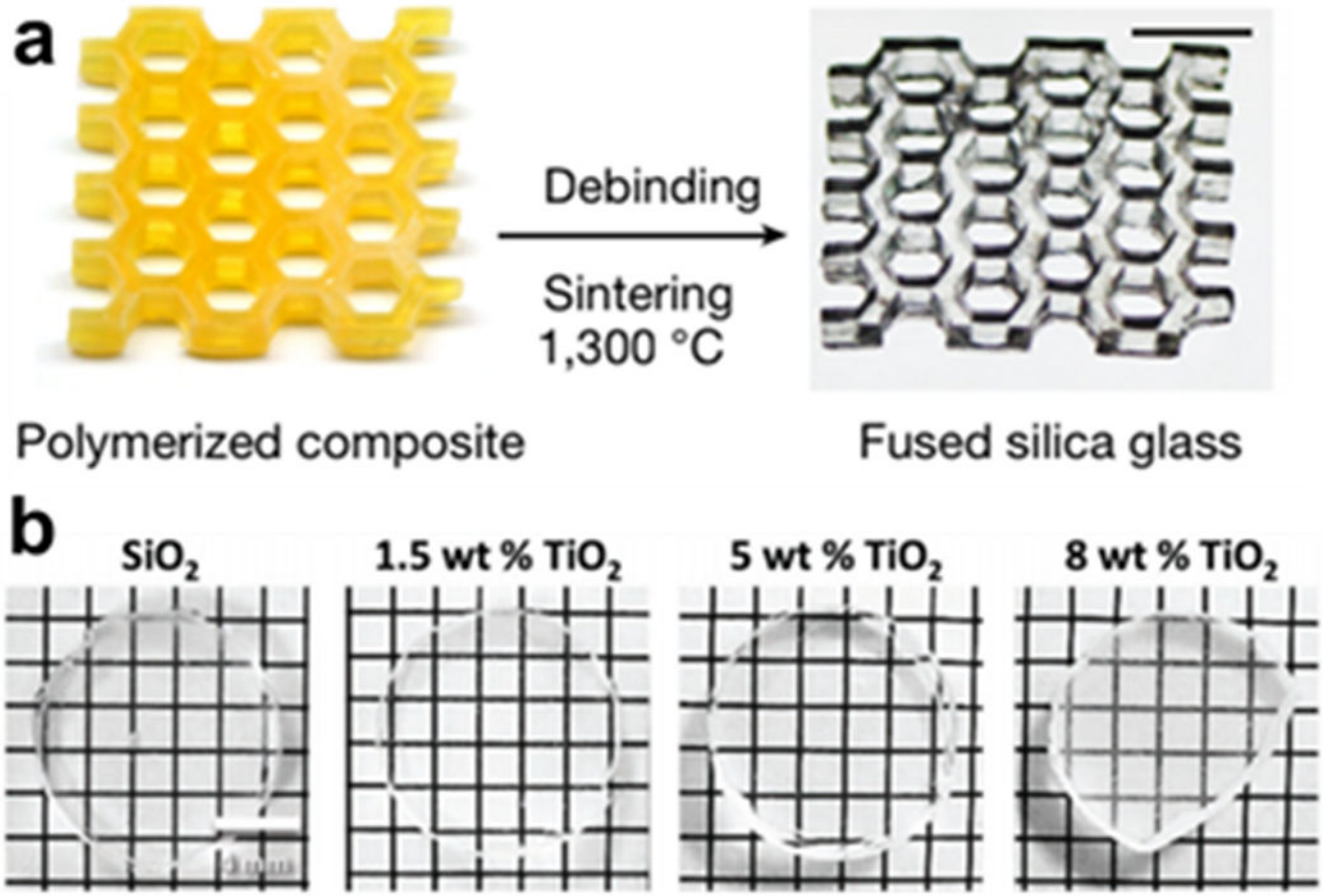

Figure 9.

3D-printed glass structures. (a) Final 2-step procedure of manufacture of fused silica glass from 3D-printed yellow scaffold mixture of HEMA and silica nanoparticles (Reprinted with permission from ref 103 Copyright 2017 Springer). (b) Printed glass doped with TiO_2 to modify the refractive index. reservoirs (Reprinted with permission from ref 105 Copyright 2018 Wiley).

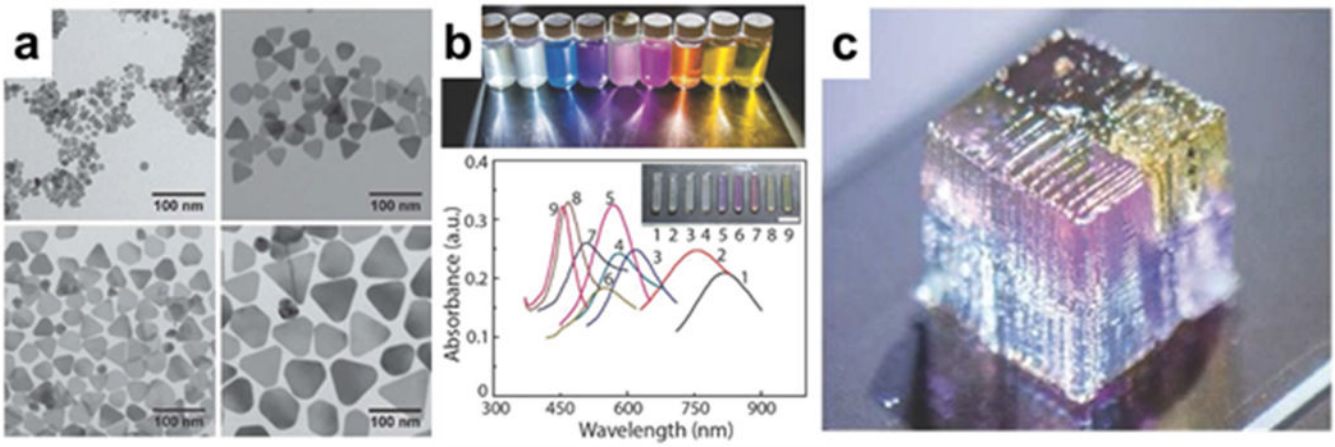

Figure 10.

(a) Plasmonic Ag nanoparticles of varying size suspended in (b) a printable gel ink before 3D printing into (c) an object of multiple plasmonic characteristics (Reprinted with permission from ref 110 Copyright 2017 Wiley).

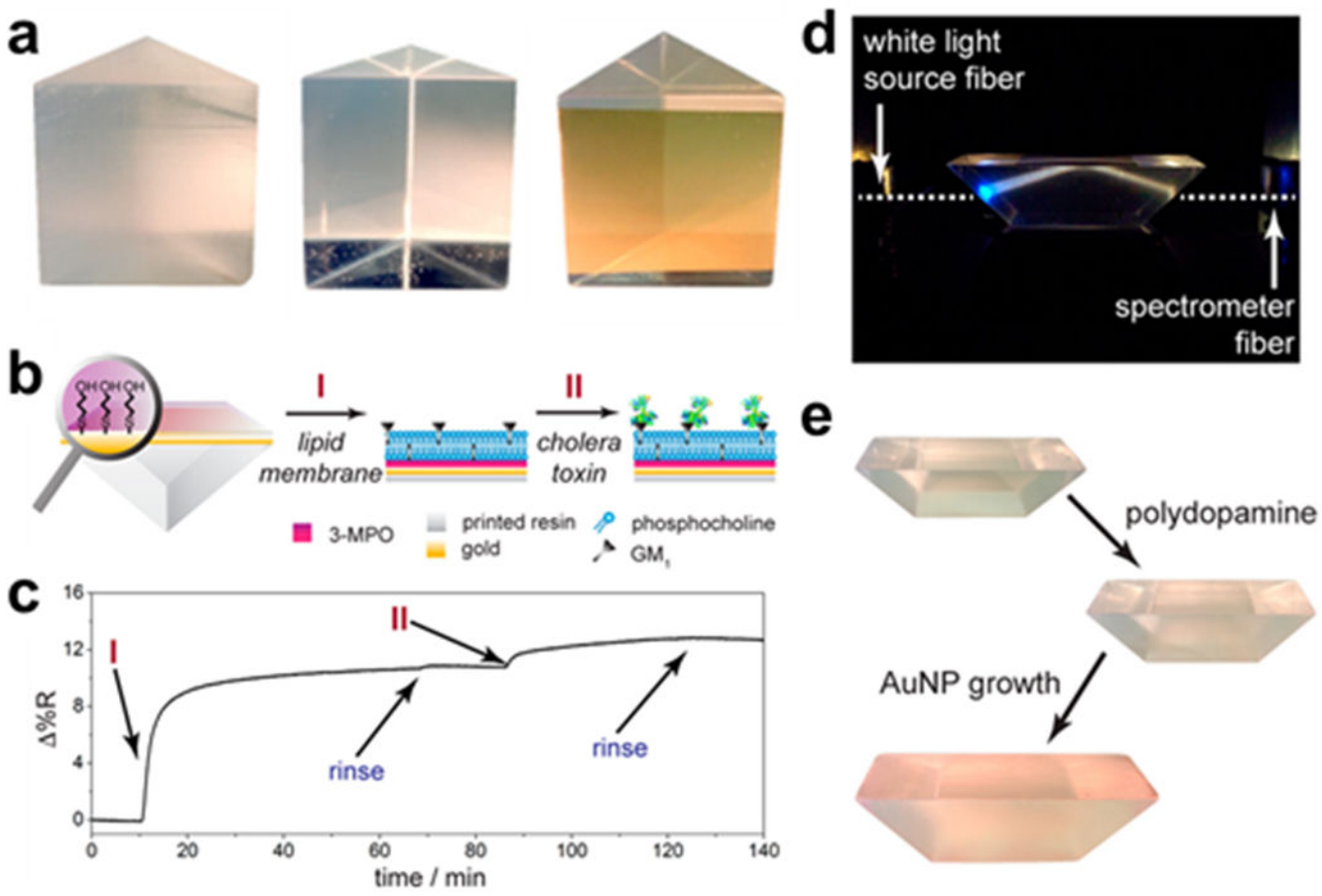

Figure 11.

3D-printed prisms with plasmonic Au surfaces. (a) Equilateral prism just-printed (left), after polishing (middle), and after Au deposition (right). (b) SPR sensing scheme with cholera toxin and GM_1 and (c) corresponding SPR sensorgram. (d) Dove prism used in single-axis SPR configuration and (e) AuNP growth on dove prism. (Reprinted with permission from ref 92 Copyright 2017 American Chemical Society).

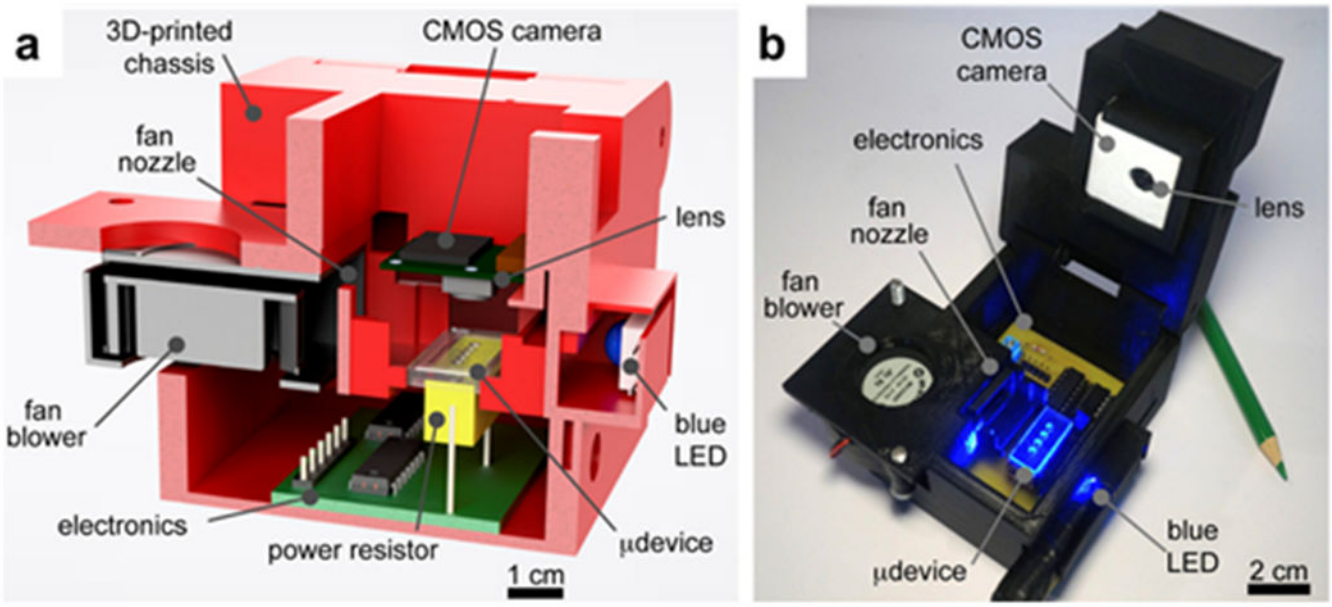

Figure 12.

(a) A representative cross section of the 3D printed PCR thermocycler, demonstrating the size and position of the parts and (b) a photograph of the instrument. (Reprinted with permission from ref 127 Copyright 2018 American Chemical Society).

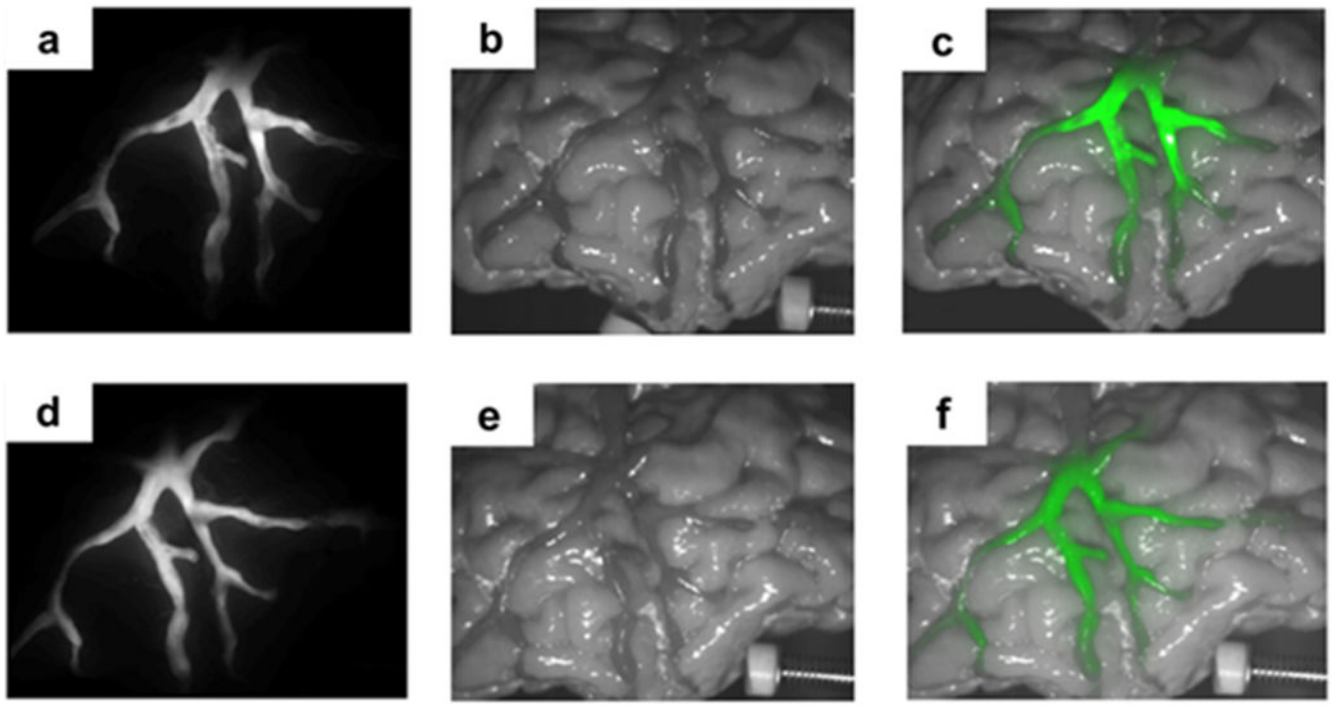

Figure 13.

The fluorescence image overlayed onto the image of the 3D printed biomimetic phantom. The phantom is filled with ICG (a,b,c) or IR800 (d,e,f) (Reprinted with permission from ref 128 Copyright 2018 Optical Society of America).

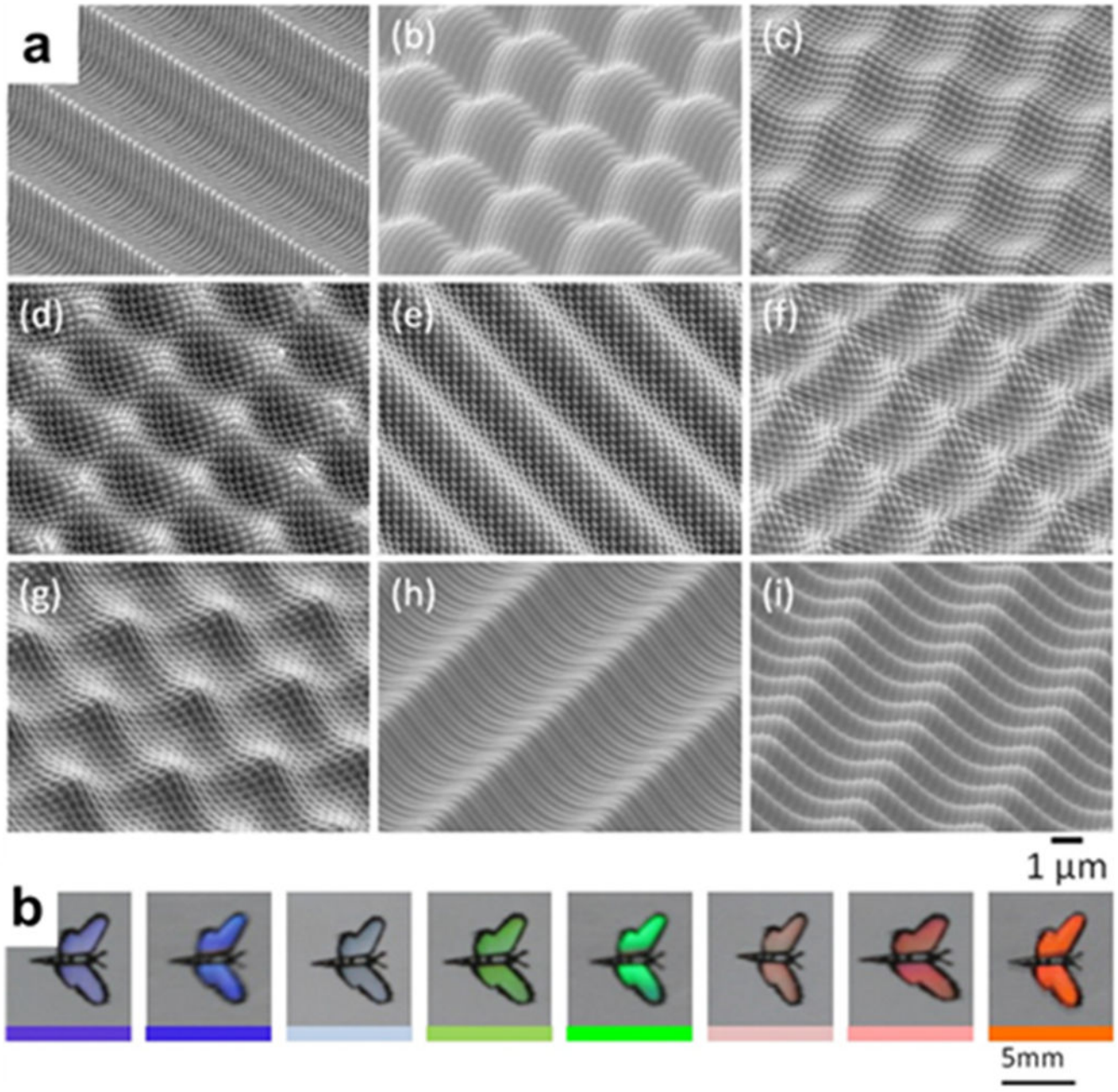

Figure 14.
3D-printed diffraction grating. As the viewing angle changes, the color of the biomimetic butterfly's wings will change color. (Reprinted with permission from ref 18 Copyright 2017 Wiley).